

PHASE PORTRAITS OF INTEGRABLE QUADRATIC SYSTEMS WITH AN INVARIANT PARABOLA AND AN INVARIANT STRAIGHT LINE

JAUME LLIBRE¹ AND MAURÍCIO FRONZA DA SILVA²

ABSTRACT. We classify the phase portraits of the quadratic polynomial differential systems having an invariant parabola, an invariant straight line, and a Darboux first integral produced by these two invariant curves.

1. INTRODUCTION AND STATEMENT OF MAIN RESULTS

Consider planar polynomial differential systems of the form

$$(1) \quad \dot{x} = P(x, y), \quad \dot{y} = Q(x, y),$$

where P and Q are real polynomials defined in \mathbb{R}^2 . The dot denotes derivative with respect to the independent variable t . The *degree* of system (1) is the maximum of the degrees of the polynomials P and Q . When a polynomial differential system (1) has degree two we call it simply a *quadratic system*.

Let U be a dense and open subset of \mathbb{R}^2 . A *first integral* of a differential system (1) is a non-locally constant \mathcal{C}^1 function $H : U \rightarrow \mathbb{R}$ which is constant on the orbits of the system (1) contained in U , i.e. H satisfies

$$(2) \quad \frac{\partial H}{\partial x}(x, y)P(x, y) + \frac{\partial H}{\partial y}(x, y)Q(x, y) = 0$$

in the points $(x, y) \in U$. We say that a quadratic system is *integrable* if it has a first integral $H : U \rightarrow \mathbb{R}$.

After the linear differential systems in the plane, i.e. the polynomial differential systems of degree one, the quadratic systems are the easier ones and they have been studied intensively, and more than one thousand papers have been published on those systems, see the references quoted in the books of Ye [24, 25] and Reyn [20]. But the classification of all the integrable quadratic system is an open problem.

The *phase portrait* of a differential system is the decomposition of its domain of definition as union of all its oriented orbits. The phase portraits

2010 *Mathematics Subject Classification*. Primary 34C05.

Key words and phrases. quadratic system, phase portraits, invariant parabola, invariant straight line.

of a polynomial differential system is drawn in the Poincaré disc which, roughly speaking, is the closed disc centered at the origin of coordinates with radius one, the interior of this disc is diffeomorphic to \mathbb{R}^2 and its boundary \mathbb{S}^1 corresponds to the infinity of \mathbb{R}^2 , each point of \mathbb{S}^1 provides a direction for going or coming from infinity. For more details see section 3 or Chapter 5 of [7].

Many classes of integrable quadratic systems have been studied, and for these classes the topological phase portraits of their quadratic systems have been classified in the Poincaré disc. A relatively easy class of integrable quadratic systems is formed by the homogeneous quadratic systems studied by Lyagina [16], Markus [17], Korol [11], Sibirskii and Vulpe [22], Newton [18], Date [5] and Vdovina [23],... An important class of integrable quadratic systems are the ones with centers studied by many authors see for instance Dulac [6], Kapteyn [9, 10], Bautin [3], Lunkevich and Sibirskii [15], Schlomiuk [21], Vulpe [27], Zoładek [28], Ye and Ye [26], Artés, Llibre and Vulpe [2], ... In general all polynomial differential systems having a center with purely imaginary eigenvalues are integrable, see for instance Poincaré [19] and Liapunov [12], and one example in [13]. Another interesting class is the one formed by the Hamiltonian quadratic systems, see Artés and Llibre [1], Kalin and Vulpe [8] and Artés, Llibre and Vulpe [2].

We say that the algebraic curve $f(x, y) = 0$ is *invariant* by the polynomial system (1) if

$$(3) \quad \frac{\partial f}{\partial x}P(x, y) + \frac{\partial f}{\partial y}Q(x, y) = K(x, y)f(x, y),$$

for some polynomial $K(x, y)$, this polynomial is called the *cofactor* of the invariant algebraic curve $f(x, y) = 0$. Note that an invariant algebraic curve of system (1) is formed by orbits of that system.

Recently the topological phase portraits in the Poincaré disc of a new class of integrable quadratic systems having an invariant ellipse and an invariant straight line have been classified in [16].

The objective of this paper is to classify the topological phase portraits in the Poincaré disc of a class of integrable quadratic systems having an invariant parabola and an invariant straight line. After an affine change of variables we may suppose without loss of generality that the equation of the invariant parabola and the one of the invariant straight line are $y = x^2$ and $ax + by + c = 0$ respectively, where a, b and c are constants such that $a^2 + b^2 \neq 0$.

More precisely we shall classify the topological phase portraits in the Poincaré disc of the class of quadratic systems

$$(4) \quad \begin{aligned} \dot{x} &= b\lambda_1(y - x^2) - \lambda_2(ax + by + c), \\ \dot{y} &= -a\lambda_1(y - x^2) - 2\lambda_2x(ax + by + c), \end{aligned}$$

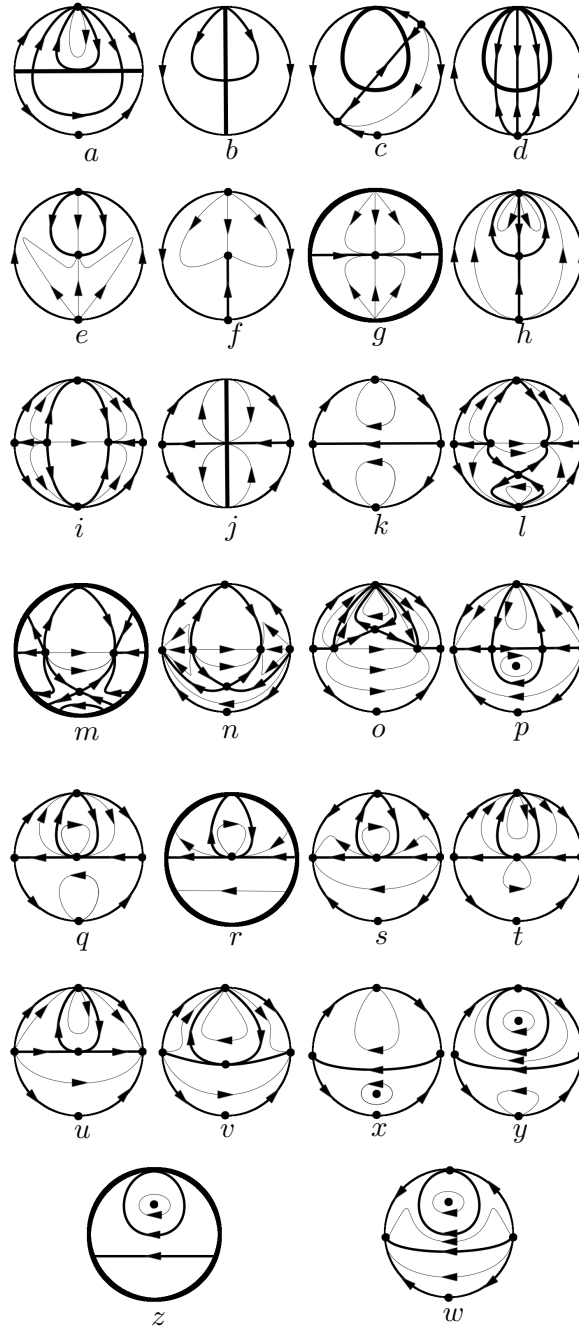


FIGURE 1. Phase portraits of systems (4) in the Poincaré disc.

where a, b, c, λ_1 and λ_2 are real parameters such that $a^2 + b^2 \neq 0$, and $\lambda_1^2 + \lambda_2^2 \neq 0$ otherwise we will have the null differential system. Note that system (4) depends on five parameters.

It is easy to check using the definition of invariant algebraic curve (3) that the quadratic systems (4) have the invariant parabola $y - x^2 = 0$ and the invariant straight line $ax + by + c = 0$. At the end of section 2 we will show that the quadratic systems (4) is a subclass of all quadratic systems having an invariant parabola and an invariant straight line.

Using the Darboux theory (see Theorem 8.7 of [7]) it is easy to obtain that

$$(5) \quad H(x, y) = (y - x^2)^{-\lambda_2} (ax + by + c)^{\lambda_1}.$$

is a first integral of the system (4) in the open and dense subset of \mathbb{R}^2 where it is defined. In fact it is immediate to check that it is a first integral using the definition (2). The existence of this first integral shows that the quadratic systems have no limit cycles.

Theorem 1. *The phase portraits in the Poincaré disc of systems (4) with $(\lambda_1^2 + \lambda_2^2)(a^2 + b^2) \neq 0$ are topologically equivalent to one of the 26 phase portraits shown in Figure 1. The correspondence between systems (4) and the phase portraits of Figure 1 are provided in Table 1.*

This work is organized as follows. In section 2 mainly we present the definitions concerning the classification of singularities of planar vector fields. In section 3 we introduce the Poincaré compactification. We perform the study of the singularities of system (4) in sections 4 and 5. Finally in section 6 we prove Theorem 1.

2. PRELIMINARY DEFINITIONS AND RESULTS

Consider a vector field $X : U \rightarrow \mathbb{R}^2$ defined on the open subset U of \mathbb{R}^2 and denote the Jacobian matrix of X at $(x, y) \in U$ by $DX(x, y)$. Let $(x_0, y_0) \in U$ be a singularity of X . We say that (x_0, y_0) is *elementary* if one of the following three conditions holds: either the real part of both eigenvalues of $DX(x_0, y_0)$ are different of zero, in this case (x_0, y_0) is a *hyperbolic singular point*; or the eigenvalues of $DX(x_0, y_0)$ are purely imaginary and (x_0, y_0) is a focus or a center; or only one of the eigenvalues of $DX(x_0, y_0)$ is different of zero, in this case (x_0, y_0) is a *semi-hyperbolic singular point*. If both eigenvalues of $DX(x_0, y_0)$ are zero then (x_0, y_0) is a *non-elementary singular point* of X .

The topological classification of the flow near a hyperbolic or semi-hyperbolic singular point of X is given, for instance in Theorems 2.15 and 2.19 of [7], respectively.

Suppose that (x_0, y_0) is a non-elementary singular point of X . If the matrix $DX(x_0, y_0)$ is not zero, then (x_0, y_0) is a *nilpotent singularity*. If $DX(x_0, y_0)$ is the zero matrix then (x_0, y_0) is a *linearly zero singularity*. The topological classification of a nilpotent singular point is given, for instance in Theorem

Global Phase Portrait of Figure 1	Parameters of system (4)
<i>a</i>	$\lambda_1 = 0$ and $b\lambda_2 \neq 0$.
<i>b</i>	$\lambda_1 = 0, b = 0$ and $a\lambda_2 \neq 0$.
<i>c</i>	$\lambda_2 = 0$ and $b\lambda_1 \neq 0$.
<i>d</i>	$\lambda_2 = 0, b = 0$ and $a\lambda_1 \neq 0$.
<i>e</i>	$a\lambda_1 > 0, a\lambda_2 > 0, b = 0$ and $a(\lambda_1 - 2\lambda_2) > 0$ or $a\lambda_1 < 0, a\lambda_2 < 0, b = 0$ and $a(\lambda_1 - 2\lambda_2) < 0$.
<i>f</i>	$a\lambda_1 > 0, a\lambda_2 > 0, b = 0$ and $a(\lambda_1 - 2\lambda_2) < 0$ or $a\lambda_1 < 0, a\lambda_2 < 0, b = 0$ and $a(\lambda_1 - 2\lambda_2) > 0$.
<i>g</i>	$a\lambda_1 > 0, a\lambda_2 > 0, b = 0$ and $\lambda_1 = 2\lambda_2$ or $a\lambda_1 < 0, a\lambda_2 < 0, b = 0$ and $\lambda_1 = 2\lambda_2$.
<i>h</i>	$a\lambda_1 > 0, a\lambda_2 < 0, b = 0$ and $a(\lambda_1 - 2\lambda_2) > 0$ or $a\lambda_1 < 0, a\lambda_2 > 0, b = 0$ and $a(\lambda_1 - 2\lambda_2) < 0$.
<i>i</i>	$\lambda_1 = \lambda_2 \neq 0, b \neq 0$ and $a^2 - 4bc > 0$.
<i>j</i>	$\lambda_1 = \lambda_2 \neq 0, b \neq 0$ and $a^2 - 4bc = 0$.
<i>k</i>	$\lambda_1 = \lambda_2 \neq 0, b \neq 0$ and $a^2 - 4bc < 0$.
<i>l</i>	$0 < \lambda_2 < \lambda_1 < 2\lambda_2, b \neq 0$ and $a^2 - 4bc > 0$ or $2\lambda_2 < \lambda_1 < \lambda_2 < 0, b \neq 0$ and $a^2 - 4bc > 0$.
<i>m</i>	$0 < 2\lambda_2 = \lambda_1, b \neq 0$ and $a^2 - 4bc > 0$ or $\lambda_1 = 2\lambda_2 < 0, b \neq 0$ and $a^2 - 4bc > 0$.
<i>n</i>	$0 < 2\lambda_2 < \lambda_1, b \neq 0$ and $a^2 - 4bc > 0$ or $\lambda_1 < 2\lambda_2 < 0, b \neq 0$ and $a^2 - 4bc > 0$.
<i>o</i>	$0 < \lambda_1 < \lambda_2, b \neq 0$ and $a^2 - 4bc > 0$ or $\lambda_2 < \lambda_1 < 0, b \neq 0$ and $a^2 - 4bc > 0$.
<i>p</i>	$\lambda_1\lambda_2 < 0, b \neq 0$ and $a^2 - 4bc > 0$.
<i>q</i>	$0 < \lambda_2 < \lambda_1 < 2\lambda_2, b \neq 0$ and $a^2 - 4bc = 0$ or $2\lambda_2 < \lambda_1 < \lambda_2 < 0, b \neq 0$ and $a^2 - 4bc = 0$.
<i>r</i>	$0 < 2\lambda_2 = \lambda_1, b \neq 0$ and $a^2 - 4bc = 0$ or $\lambda_1 = 2\lambda_2 < 0, b \neq 0$ and $a^2 - 4bc = 0$.
<i>s</i>	$0 < 2\lambda_2 < \lambda_1, b \neq 0$ and $a^2 - 4bc = 0$ or $\lambda_1 < 2\lambda_2 < 0, b \neq 0$ and $a^2 - 4bc = 0$.
<i>t</i>	$0 < \lambda_1 < \lambda_2, b \neq 0$ and $a^2 - 4bc = 0$ or $\lambda_2 < \lambda_1 < 0, b \neq 0$ and $a^2 - 4bc = 0$.
<i>u</i>	$\lambda_1\lambda_2 < 0, b \neq 0$ and $a^2 - 4bc = 0$.
<i>v</i>	$\lambda_1\lambda_2 < 0, b \neq 0$ and $a^2 - 4bc < 0$.
<i>x</i>	$0 < \lambda_1 < \lambda_2, b \neq 0$ and $a^2 - 4bc < 0$ or $\lambda_2 < \lambda_1 < 0, b \neq 0$ and $a^2 - 4bc < 0$.
<i>y</i>	$0 < \lambda_2 < \lambda_1 < 2\lambda_2, b \neq 0$ and $a^2 - 4bc < 0$ or $2\lambda_2 < \lambda_1 < \lambda_2 < 0, b \neq 0$ and $a^2 - 4bc < 0$.
<i>z</i>	$0 < 2\lambda_2 = \lambda_1, b \neq 0$ and $a^2 - 4bc < 0$ or $\lambda_1 = 2\lambda_2 < 0, b \neq 0$ and $a^2 - 4bc < 0$.
<i>w</i>	$0 < 2\lambda_2 < \lambda_1, b \neq 0$ and $a^2 - 4bc < 0$ or $\lambda_1 < 2\lambda_2 < 0, b \neq 0$ and $a^2 - 4bc < 0$.

TABLE 1. Classification of the phase portraits in the Poincaré disc of the quadratic systems (4).

3.5 of [7]. The main tool used for studying the local phase portraits of the the linearly zero singularities are the changes of variables called blow-ups.

In general a *quasi-homogeneous blow-up* is a change of variables of the form

$$\begin{aligned}(x, y) &\mapsto (x^\alpha, x^\beta y), \text{ positive } x\text{-direction,} \\ (x, y) &\mapsto (-x^\alpha, x^\beta y), \text{ negative } x\text{-direction,} \\ (x, y) &\mapsto (xy^\alpha, y^\beta), \text{ positive } y\text{-direction,} \\ (x, y) &\mapsto (xy^\alpha, -y^\beta), \text{ negative } y\text{-direction,}\end{aligned}$$

where α, β are positive integers. For quasi-homogeneous blow-ups in the x -direction (respectively y -direction), when α (respectively β) is odd, the information obtained in the positive x -direction (respectively y -direction) is useful to the negative x -direction (respectively y -direction). A suitable choice of α and β avoids successive homogeneous blow-up's (see p. 104 of [7]).

In this work, all isolated singularities are hyperbolic, nilpotent, or linearly zero. The classification of nilpotent singularities could be perform using Theorem 3.5 of [7]. But in order to obtain information on the localization of the separatrices of the nilpotent singularities we will use quasi-homogeneous blow-ups (see Lemmas 10 and 15).

For showing that the class of quadratic systems (4) having the invariant parabola $y = x^2$, the invariant straight line $ax + by + c = 0$, and the first integral (5) are not all the quadratic systems having the invariant parabola $y = x^2$ and the invariant straight line $ax + by + c = 0$, it is sufficient to provide an example. Consider the invariant straight line

$$L = ax + by + c = 8x + 16y + 1 = 0,$$

and the subclass of quadratic systems (4) having this invariant straight line are

$$(6) \quad \begin{aligned}\dot{x} &= 16\lambda_1(y - x^2) - \lambda_2(8x + 16y + 1), \\ \dot{y} &= -8\lambda_1(y - x^2) - 2\lambda_2x(8x + 16y + 1).\end{aligned}$$

But the quadratic system

$$\begin{aligned}\dot{x} &= 1 + 3x + 33y - 36x^2 + 4xy, \\ \dot{y} &= 2(x - 4y + 7x^2 - 3xy + 4y^2).\end{aligned}$$

also has the invariant parabola $y = x^2$ with cofactor $k_P = -8(1 + 9x - y)$ and the invariant straight line L with cofactor $k_L = 8(1 - x + y)$, it is not contained in the subclass and it has no a first integral of the form (5), because according statement (i) of Theorem 8.7 of [7] such a first integral only exists if there are real numbers μ_1 and μ_2 not all zero such that

$$\mu_1 k_P + \mu_2 k_L = -8\mu_1(1 + 9x - y) + 8\mu_2(1 - x + y) = 0,$$

but these μ_1 and μ_2 do not exist.

3. THE POINCARÉ COMPACTIFICATION

The Poincaré compactification is a helpful technique to study the behavior near the infinity of a polynomial vector field defined in \mathbb{R}^2 . In this section X is the planar polynomial vector field defined by the polynomial differential system (1) of degree d .

We shall use the notation $\mathbb{S}^2 = \{(z_1, z_2, z_3) \in \mathbb{R}^3; z_1^2 + z_2^2 + z_3^2 = 1\}$ and $\mathbb{S}^1 = \{(z_1, z_2, z_3) \in \mathbb{S}^2; z_3 = 0\}$ for the two-dimensional sphere and its equator, respectively. We identify \mathbb{R}^2 with the tangent plane π of \mathbb{S}^2 at the point $(0, 0, 1)$. Considering the central projection from π into \mathbb{S}^2 , we obtain a vector field X' on $\mathbb{S}^2 \setminus \mathbb{S}^1$ such that the infinity points of π are projected in \mathbb{S}^1 .

Observe that the vector field X' is symmetric with respect to the center of \mathbb{S}^2 . X' is an unbounded vector field near \mathbb{S}^1 , but after a multiplication by an appropriate factor, the resultant vector field $p(X)$, called the *Poincaré compactification* of X , is analytic and defined in the whole sphere \mathbb{S}^2 . The symmetry means that it is sufficient to consider $p(X)$ defined only in the closed northern hemisphere H of \mathbb{S}^2 . We project the vector field $p(X)$ on H using the orthogonal projection into a vector field on the disc $\{(z_1, z_2, z_3) \in \mathbb{R}^3; z_1^2 + z_2^2 \leq 1, z_3 = 0\}$, called the *Poincaré disc*. It is on this disc where we draw the phase portraits of the polynomial differential systems, its interior is diffeomorphic to \mathbb{R}^2 and its boundary \mathbb{S}^1 corresponds to the infinity of \mathbb{R}^2 .

To obtain an explicit expression of the Poincaré compactification $p(X)$, the northern and the southern hemisphere of \mathbb{S}^2 are denoted by $H^+ = \{(z_1, z_2, z_3) \in \mathbb{S}^2; z_3 > 0\}$ and $H^- = \{(z_1, z_2, z_3) \in \mathbb{S}^2; z_3 < 0\}$, respectively. We consider the central projections of $\pi := \{(z_1, z_2, z_3) \in \mathbb{R}^3; z_3 = 1\}$ in H^+ and H^- , which are defined by

$$\begin{aligned} f^+ : \pi &\rightarrow H^+ & f^- : \pi &\rightarrow H^- \\ z &\mapsto \frac{1}{\Delta(z)}(z_1, z_2, 1) & \text{and} & z &\mapsto \frac{1}{\Delta(z)}(-z_1, -z_2, -1) \end{aligned}$$

respectively. Here $\Delta(z) = \sqrt{z_1^2 + z_2^2 + 1}$, $z \in \pi$. Define the vector field X' on $\mathbb{S}^2 \setminus \mathbb{S}^1$ by

$$X'(w) = \begin{cases} Df^+(z)X(z) & \text{if } w = f^+(z), \\ Df^-(z)X(z) & \text{if } w = f^-(z). \end{cases}$$

The vector field X' is unbounded in a neighborhood of \mathbb{S}^1 , but the vector field $w_3^d X'(w)$ is an analytical extension of X' to the whole \mathbb{S}^2 . This extension is the *Poincaré compactification* of X that we have denoted by $p(X)$.

In general, the vector field $p(X)$ is C^ω -equivalent, but not C^ω -conjugated, to X in each hemisphere of \mathbb{S}^2 . Then we study the trajectories of X near a singularity using the correspondent singularities of $p(X)$. Since $p(X)$ may

has singularities in \mathbb{S}^1 , a singular point of $p(X)$ which belongs to $\mathbb{S}^2 \setminus \mathbb{S}^1$ or to \mathbb{S}^1 is called *finite* or *infinite* singular point of X , respectively.

We can prove that \mathbb{S}^1 is invariant under the flow of $p(X)$. Using the expressions of f^+ and f^- we obtain that $p(X)$ is symmetric with respect to the origin, then it is sufficient to study the trajectories of $p(X)$ in $H^+ \cup \mathbb{S}^1$.

We will obtain the expressions of $p(X)$ in the local charts of \mathbb{S}^2 . For $j = 1, 2, 3$ consider $U_j = \{(z_1, z_2, z_3) \in \mathbb{S}^2; z_j > 0\}$, $V_j = \{(z_1, z_2, z_3) \in \mathbb{S}^2; z_j < 0\}$ and $\varphi_j : U_j \rightarrow \mathbb{R}^2$, $\psi_j : V_j \rightarrow \mathbb{R}^2$ defined by

$$\varphi_1(z) = -\psi_1(z) = \frac{(z_2, z_3)}{z_1}, \quad \varphi_2(z) = -\psi_2(z) = \frac{(z_1, z_3)}{z_2}, \quad \varphi_3(z) = \frac{(z_1, z_2)}{z_3}.$$

We denote by (u, v) the value of φ_j or ψ_j at the point z . The expression of $p(X)$ in the chart (U_1, φ_1) is

$$\dot{u} = v^d \left[-uP \left(\frac{1}{v}, \frac{u}{v} \right) + Q \left(\frac{1}{v}, \frac{u}{v} \right) \right], \quad \dot{v} = -v^{d+1} P \left(\frac{1}{v}, \frac{u}{v} \right).$$

The expression of $p(X)$ in the chart (U_2, φ_2) is

$$\dot{u} = v^d \left[P \left(\frac{u}{v}, \frac{1}{v} \right) - uQ \left(\frac{u}{v}, \frac{1}{v} \right) \right], \quad \dot{v} = -v^{d+1} Q \left(\frac{u}{v}, \frac{1}{v} \right),$$

and the expression of $p(X)$ in the chart (U_3, φ_3) is

$$\dot{u} = P(u, v), \quad \dot{v} = Q(u, v).$$

The expression of $p(X)$ in the chart (V_j, ψ_j) is the expression of $p(X)$ in the chart (U_j, φ_j) multiplied by $(-1)^{d-1}$, for $j = 1, 2$ and 3 .

Notice that $(u, v) \in U_j$ is an infinite singular point of X if and only if the expression of $p(X)$ in the chart (U_j, φ_j) vanishes at (u, v) and $v = 0$.

Due to the symmetry of $p(X)$ with respect to the origin of coordinates, if z is an infinite singular point of X then $-z$ is also an infinite singular point of X . Then we only need to study $p(X)$ in the charts (U_j, φ_j) , $j = 1, 2, 3$.

If z is an infinite singular point of X with $z \in U_2$ and $z \neq (0, 0, 0)$ then $z \in U_1 \cup V_1$. Then, to study all the infinite singular points of $p(X)$, it is sufficient to study the singularities of $p(X)$ in U_1 and the origin of U_2 .

From the definition of the Poincaré compactification follows Remarks 2-4.

Remark 2. Suppose that $k : \mathbb{R}^2 \rightarrow \mathbb{R}$ is a polynomial function of degree d_1 and \tilde{X} is a polynomial planar vector field with degree d_2 . Define $X = k\tilde{X}$. Let $p_j(X)$ and $p_j(\tilde{X})$ the expression of X and \tilde{X} in the chart (U_j, φ_j) , respectively, for $j = 1$ and 2 . Then

$$p_1(X) = v^{d_1} k \left(\frac{1}{v}, \frac{u}{v} \right) p_1(\tilde{X}) \quad \text{and} \quad p_2(X) = v^{d_1} k \left(\frac{u}{v}, \frac{1}{v} \right) p_2(\tilde{X}).$$

Remark 3. If $b \neq 0$ then the points of \mathbb{R}^2 of the straight line $ax + by + c = 0$ of \mathbb{R}^2 are mapped into the points of $\{a + bu + cv = 0\} \cap U_1$ with $v \neq 0$. Observe that the straight line $a + bu + cv = 0$ cuts the line of the infinity $v = 0$ at the point $(-a/b, 0)$.

Remark 4. If $b = 0$ then the points of \mathbb{R}^2 of the straight line $ax + by + c = 0$ of \mathbb{R}^2 are mapped into the points $\{au + cv = 0\} \cap U_2$ with $v \neq 0$. Observe that the straight line $au + cv = 0$ cuts the line of the infinity $v = 0$ at the point $(0, 0)$.

Remark 5. For each $k \in \mathbb{R}$ the points of \mathbb{R}^2 of the parabola $y = x^2 + k$ contained in the half-planes $y > 0$ or $y < 0$ are mapped into the points of the form $v = u^2 + kv^2$ of U_2 , or into the points of the form $-v = u^2 + kv^2$ of V_2 , respectively.

4. PHASE PORTRAITS OF SYSTEM (4) FOR THE CASE $\lambda_1 \lambda_2 = 0$ AND $\lambda_1^2 + \lambda_2^2 \neq 0$.

In this section we present the phase portrait in the Poincaré disc of system (4) for the case $\lambda_1 \lambda_2 = 0$. If $\lambda_1 = \lambda_2 = 0$ and $\lambda_1^2 + \lambda_2^2 \neq 0$.

Lemma 6. Suppose that $\lambda_1 = 0$ and $\lambda_2 \neq 0$. If $b \neq 0$ or $b = 0$ then the phase portrait in the Poincaré disc of system (4) is shown in Figures 1-a or 1-b, respectively.

Proof. After the rescaling given by $ds = \lambda_2(ax + by + c) dt$ system (4) becomes

$$(7) \quad x' = -1, \quad y' = -2x,$$

where the prime denotes the derivative with respect to the variable s . The phase portrait in \mathbb{R}^2 of system (7) is given in Figure 2-a.

The expression of the Poincaré compactification of system (7) in the charts (U_1, φ_1) and (U_2, φ_2) is

$$(8) \quad \dot{u} = uv - 2, \quad \dot{v} = v^2,$$

and

$$(9) \quad \dot{u} = 2u^2 - v, \quad \dot{v} = 2uv,$$

respectively. We present the phase portrait of system (8) in a sufficiently small neighborhood of the axis $v = 0$ in Figure 2-b.

Each orbit of system (7) is contained in a parabola given by $y = x^2 + k$, for an appropriated choice of $k \in \mathbb{R}$. From Remark 5 it follows that the phase portrait of system (9) is the one of Figure 2-c.

Combining the informations of Figure 2-a-c we obtain the phase portrait in the Poincaré disc of system (7) in Figure 2-d. Using Remark 2 with $k(x, y) = \lambda_2(ax + by + c)$ and $\tilde{X} = (-1, -2x)$ we obtain the conclusions of Lemma 6. \square

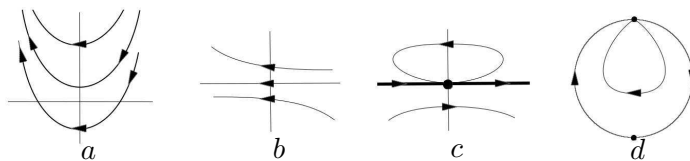


FIGURE 2. (a) Phase portrait in \mathbb{R}^2 of system (7). (b) Phase portrait of system (8) in a neighborhood of the axis $v = 0$. (c) Phase portrait of system (9). (d) Phase portrait in the Poincaré disc of system (7).

Lemma 7. *Suppose that $\lambda_1 \neq 0$ and $\lambda_2 = 0$. If $b \neq 0$ or $b = 0$ then the phase portrait in the Poincaré disc of system (4) is given in Figures 1-c or 1-d, respectively.*

Proof. After the rescaling given by $ds = \lambda_1(y - x^2) dt$ system (4) becomes

$$(10) \quad x' = b, \quad y' = -a.$$

The phase portrait in \mathbb{R}^2 of system (10) is shown in Figure 3.

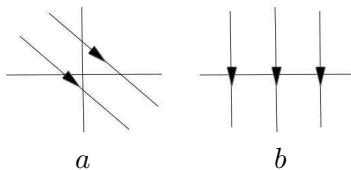


FIGURE 3. Phase portrait of system (10). (a) $b > 0$; if $b < 0$ then the orientation of the orbits is reversed. (b) $b = 0$ and $a > 0$; if $b = 0$ and $a < 0$ then the orientation of the orbits is reversed.

The expression of the Poincaré compactification of system (10) in the charts (U_1, φ_1) and (U_2, φ_2) is

$$(11) \quad \dot{u} = -(a + bu), \quad \dot{v} = -bv,$$

and

$$(12) \quad \dot{u} = au + b, \quad \dot{v} = av,$$

respectively.

We present the phase portrait of systems (11) and (12) in Figures 4-a-d.

Combining the informations of Figures 3 and 4 we obtain the local and the phase portrait in the Poincaré disc of system (10) in Figure 5. Using Remark 2 with $k(x, y) = \lambda_1(y - x^2)$ and $\tilde{X} = (b, -a)$ we **conclude the proof.** \square

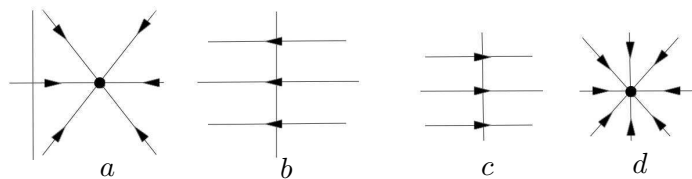


FIGURE 4. (a) Phase portrait of system (11) with $b > 0$; if $b < 0$ then the orientation of the orbits is reversed. (b) Phase portrait of system (11) with $a > 0$ and $b = 0$; if $a < 0$ and $b = 0$ then the orientation of the orbits is reversed. (c) Phase portrait of system (12) with $b > 0$; if $b < 0$ then the orientation of the orbits is reversed. (d) Phase portrait of system (12) with $a > 0$ and $b = 0$; if $a < 0$ and $b = 0$ then the orientation of the orbits is reversed.

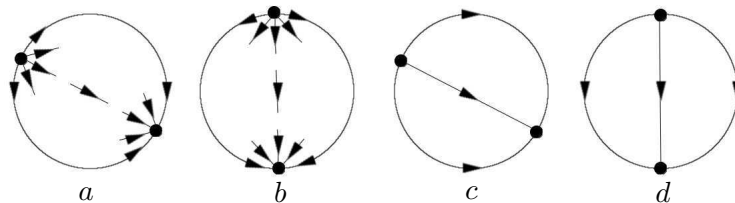


FIGURE 5. (a) Local phase portrait in the Poincaré disc of system (10) with $b > 0$; if $b < 0$ then the orientation of the orbits is reversed. (b) Local phase portrait in the Poincaré disc of system (10) with $b = 0$ and $a > 0$; if $b = 0$ and $a < 0$ then the orientation of the orbits is reversed. (c) Phase portrait in the Poincaré disc of system (10) with $b > 0$; if $b < 0$ then the orientation of the orbits is reversed. (d) Phase portrait in the Poincaré disc of system (10) with $b = 0$ and $a > 0$; if $b = 0$ and $a < 0$ then the orientation of the orbits is reversed.

5. LOCAL PHASE PORTRAITS OF SYSTEM (4) FOR THE CASE $\lambda_1\lambda_2 \neq 0$

In this section we will study the local phase portraits in the Poincaré disc of system (4) when $\lambda_1\lambda_2 \neq 0$.

5.1. Finite singularities of system (4). We denote the parabola $y = x^2$ and the straight line $ax + by + c = 0$ by p and l , respectively. In this subsection we consider the cases $b = 0; b \neq 0$ and $\lambda_1 = \lambda_2; b \neq 0$ and $\lambda_1 \neq \lambda_2$ in Lemmas 8-10, respectively.

Lemma 8. *Suppose that $\lambda_1\lambda_2 \neq 0$ and $b = 0$. Then system (4) has a unique singularity (x_0, y_0) and the local phase portrait in \mathbb{R}^2 of system (4) at (x_0, y_0) is given in Figure 6.*

Proof. From the hypothesis $a^2 + b^2 \neq 0$ it follows that $a \neq 0$. The unique singularity of system (4) is (x_0, y_0) where $x_0 = -c/a$ and $y_0 = c^2/a^2$. Observe

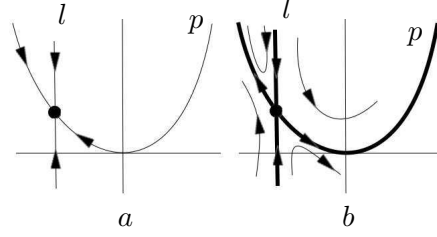


FIGURE 6. Local phase portrait of system (4). (a) $b = 0, a\lambda_1 > 0$ and $a\lambda_2 > 0$. If $b = 0, a\lambda_1 < 0$ and $a\lambda_2 < 0$ then the orientation of the orbits is reversed. (b) $b = 0, a\lambda_1 > 0$ and $a\lambda_2 < 0$. If $b = 0, a\lambda_1 < 0$ and $a\lambda_2 > 0$ then the orientation of the orbits is reversed.

that $(x_0, y_0) \in p \cap l$ and l is given by the equation $x = x_0$. Moreover $\dot{y}|_{x=x_0} = -a\lambda_1(y - y_0)$.

The eigenvalues of the Jacobian matrix of the vector field defined by system (4) evaluated at (x_0, y_0) are $-a\lambda_2$ and $-a\lambda_1$. Then (x_0, y_0) is a hyperbolic singular point. Since $(x_0, y_0) \in p \cap l$, for the saddle point case it follows the separatrices are contained in $p \cup l$. We presented the local phase portrait of system (4) in Figure 6. \square

Lemma 9. Suppose that $\lambda_1\lambda_2 \neq 0, b \neq 0$ and $\lambda_1 = \lambda_2$. The local phase portrait of system (4) is shown in Figure 7.

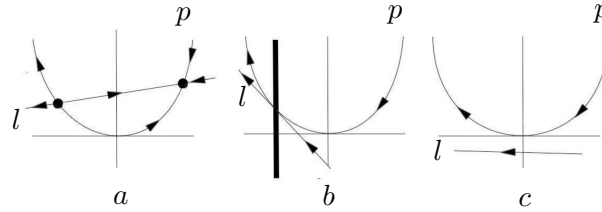


FIGURE 7. Local phase portrait of system (4). (a) $\lambda_1 = \lambda_2, b\lambda_1 > 0$ and $a^2 - 4bc > 0$. If $\lambda_1 = \lambda_2, b\lambda_1 < 0$ and $a^2 - 4bc > 0$ then the orientation of the orbits is reversed. (b) $\lambda_1 = \lambda_2, b\lambda_1 > 0$ and $a^2 - 4bc = 0$. If $\lambda_1 = \lambda_2, b\lambda_1 < 0$ and $a^2 - 4bc = 0$ then the orientation of the orbits is reversed. (c) $\lambda_1 = \lambda_2$ and $b\lambda_1 > 0$. If $\lambda_1 = \lambda_2$ and $b\lambda_1 < 0$ then the orientation of the orbits is reversed.

Proof. Taking the rescaling given by $ds = \lambda_1 dt$ system (4) becomes

$$(13) \quad x' = -bx^2 - ax - c, \quad y' = -(2bx + a)y - ax^2 - 2cx.$$

In system (13) we have $x' = 0$ if and only if $x = (a \pm \sqrt{a^2 - 4bc})/(2b)$. Then we consider three cases.

Case 1: $a^2 - 4bc > 0$. In this case system (13) has two singularities, (x_1, y_1) and (x_2, y_2) , where $x_1 = -(\sqrt{a^2 - 4bc} + a)/(2b)$, $x_2 = (\sqrt{a^2 - 4bc} - a)/(2b)$ and $y_j = x_j^2$ for $j = 1, 2$.

Observe that for $j = 1, 2$ we have $(x_j, y_j) \in p \cap l$. **The eigenvalues of the Jacobian matrix of the vector field defined by system (13) evaluated at (x_j, y_j) are equal to $(-1)^{j+1}\sqrt{a^2 - 4bc}$. Then (x_j, y_j) is a hyperbolic singular point, $j = 1, 2$.** We show the local phase portrait of system (4) at (x_1, y_1) and (x_2, y_2) in Figure 7-a.

Case 2: $a^2 - 4bc = 0$. In this case we can write system (13) into the form

$$(14) \quad x' = -b(x - x_0)^2, \quad y' = -(2by + ax)(x - x_0),$$

with $x_0 = -a/(2b)$. After the rescaling given by $d\tau = (x - x_0) dt$ system (14) becomes

$$(15) \quad \frac{dx}{d\tau} = -b(x - x_0), \quad \frac{dy}{d\tau} = -(2by + ax).$$

The singularity of system (15) is (x_0, y_0) , where $y_0 = x_0^2$. Observe that $(x_0, y_0) \in p \cap l$ and the tangent line to p at (x_0, y_0) is l .

The eigenvalues of the Jacobian matrix of the vector field defined by system (15) evaluated at (x_0, y_0) are $-b$ and $-2b$. Then (x_0, y_0) is a hyperbolic singular point of system (15). We give the local phase portrait of system (4) at (x_0, y_0) in Figure 7-b.

Case 3: $a^2 - 4bc < 0$. In this case system (4) has no singularities. We present the phase portrait of system (4) in Figure 7-c. \square

The α -limit and the ω -limit set of the orbit Γ are denoted by $\alpha(\Gamma)$ and $\omega(\Gamma)$, respectively. We say that the orbit Γ *connects* the singularities (x_1, y_1) and (x_2, y_2) when $\alpha(\Gamma) = \{(x_1, y_1)\}$ and $\omega(\Gamma) = \{(x_2, y_2)\}$; or $\alpha(\Gamma) = \{(x_2, y_2)\}$ and $\omega(\Gamma) = \{(x_1, y_1)\}$. From now on for system (4) we denote by P , N and Σ the subsets of \mathbb{R}^2 such that $\dot{x} > 0$, $\dot{x} < 0$ and $\dot{x} = 0$ respectively.

Lemma 10. *Suppose that $\lambda_1\lambda_2 \neq 0$, $b \neq 0$ and $\lambda_1 \neq \lambda_2$.*

- (a) *The local phase portrait in \mathbb{R}^2 of system (4) is given in Figures 8-11.*
- (b) *For the case of Figure 11-a, if Γ is a separatrix of the saddle point and $\Gamma \cap P \neq \emptyset$ (respect. $\Gamma \cap N \neq \emptyset$) then $\Gamma \subset P$ (respect. $\Gamma \subset N$).*

Proof. (a) Solving the equation $\dot{x} = 0$ for y and replacing the result in the equation $\dot{y} = 0$, we obtain that a point (x, y) is a singularity of system (4) when x satisfies

$$(16) \quad 2b^2\lambda_1\lambda_2x^3 + 3ab\lambda_1\lambda_2x^2 + (2bc + a^2)\lambda_1\lambda_2x + ac\lambda_1\lambda_2 = 0$$

and y is given by

$$y = -\frac{b\lambda_1x^2 + a\lambda_2x + c\lambda_2}{b(\lambda_2 - \lambda_1)}.$$

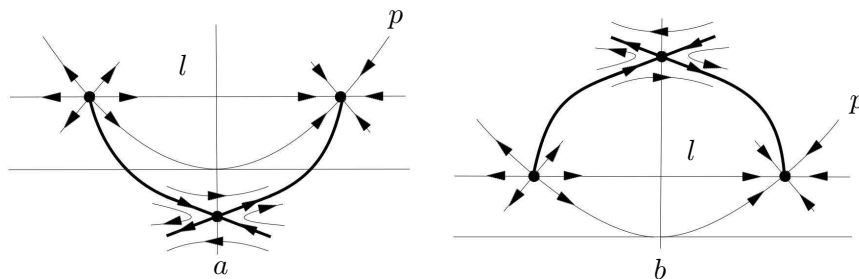


FIGURE 8. Local phase portrait of system (4) with $\lambda_1 \lambda_2 \neq 0, \lambda_1 \neq \lambda_2, b \neq 0$ and $a^2 - 4bc > 0$. (a) $\lambda_1 > \lambda_2 > 0$ and $b > 0$ or $\lambda_1 < \lambda_2 < 0$ and $b < 0$. If $\lambda_1 < \lambda_2 < 0$ and $b > 0$ or $0 < \lambda_2 < \lambda_1$ and $b < 0$ then the orientation of the orbits is reversed. (b) $0 < \lambda_1 < \lambda_2$ and $b > 0$ or $\lambda_2 < \lambda_1 < 0$ and $b < 0$. If $\lambda_2 < \lambda_1 < 0$ and $b > 0$ or $0 < \lambda_1 < \lambda_2$ and $b < 0$ then the orientation of the orbits is reversed.

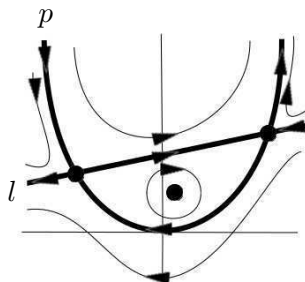


FIGURE 9. Local phase portrait of system (4) with $\lambda_1 \lambda_2 \neq 0, \lambda_1 \neq \lambda_2, b \neq 0$ and $a^2 - 4bc > 0$. The figure corresponds to cases $\lambda_2 < 0 < \lambda_1$ and $b > 0$ or $\lambda_1 < 0 < \lambda_2$ and $b < 0$. If $\lambda_1 < 0 < \lambda_2$ and $b > 0$ or $\lambda_2 < 0 < \lambda_1$ and $b < 0$ then the orientation of the orbits is reversed.

Dividing by $2b^2\lambda_1\lambda_2$ and performing the change of variables given by $x \mapsto x + a/(2b)$, equation (16) becomes

$$(17) \quad x^3 + \frac{4bc - a^2}{4b^2}x = 0.$$

Then we consider three cases.

Case 1: $a^2 > 4bc$. There exist three singularities $(x_j, y_j), j = 0, 1, 2$, of the system (4), where $x_0 = -a/(2b), x_1 = x_0 - \sqrt{a^2/b^2 - 4c/b}, x_2 = x_0 + \sqrt{a^2/b^2 - 4c/b}, y_0 = -(b\lambda_1 x_0^2 + a\lambda_2 x_0 + c\lambda_2)/(b\lambda_2 - b\lambda_1)$ and $y_j = x_j^2$ for $j = 1, 2$. Notice that $(x_j, y_j) \in p \cap l$ for $j = 1, 2$ and $(x_0, y_0) \notin p \cup l$.

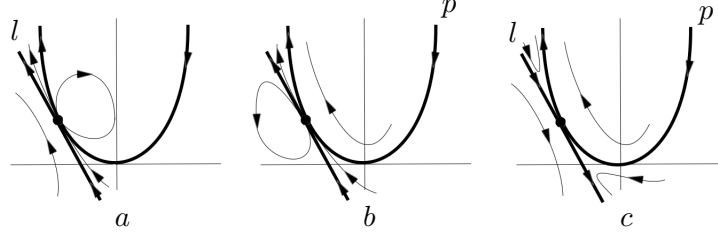


FIGURE 10. Local phase portrait of system (4) at (x_0, y_0) for the case $b\lambda_1\lambda_2(\lambda_1 - \lambda_2) \neq 0$ and $4bc = a^2$. (a) $0 < \lambda_2 < \lambda_1$ and $b > 0$ or $\lambda_1 < \lambda_2 < 0$ and $b < 0$. If $\lambda_1 < \lambda_2 < 0$ and $b > 0$ or $0 < \lambda_2 < \lambda_1$ and $b < 0$ then the orientation of the orbits is reversed. The separatrices are contained in the straight line $ax + by + c = 0$ and in the region $y \geq x^2$. (b) $0 < \lambda_1 < \lambda_2$ and $b > 0$ or $\lambda_2 < \lambda_1 < 0$ and $b < 0$. If $\lambda_2 < \lambda_1 < 0$ and $b > 0$ or $0 < \lambda_1 < \lambda_2$ and $b < 0$ then the orientation of the orbits is reversed. The separatrices are contained in region $ax + by + c \leq 0$ and parabola $y = x^2$. (c) $\lambda_1 < 0 < \lambda_2$ and $b > 0$ or $\lambda_2 < 0 < \lambda_1$ and $b < 0$. If $\lambda_2 < 0 < \lambda_1$ and $b > 0$ or $\lambda_1 < 0 < \lambda_2$ and $b < 0$ then the orientation of the orbits is reversed. The separatrices are contained in the straight line $ax + by + c = 0$ and in the parabola $y = x^2$.

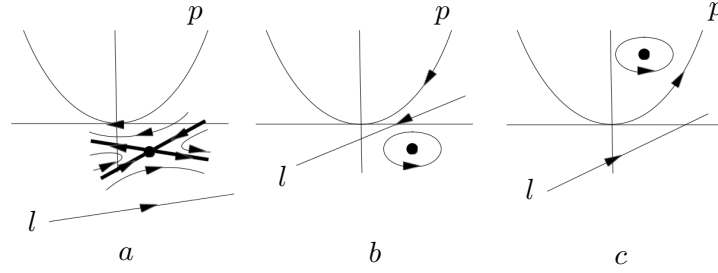


FIGURE 11. Local phase portrait of system (4) at (x_0, y_0) . (a) $\lambda_1\lambda_2 < 0, b(\lambda_1 - \lambda_2) < 0$ and $a^2 - 4bc < 0$. If $\lambda_1\lambda_2 < 0, b(\lambda_1 - \lambda_2) > 0$ and $a^2 - 4bc < 0$ then the orientation of the orbits is reversed. (b) $\lambda_1\lambda_2 > 0, b(\lambda_1 - \lambda_2) < 0, \lambda_2(\lambda_1 - \lambda_2) < 0$ and $a^2 - 4bc < 0$. If $\lambda_1\lambda_2 > 0, b(\lambda_1 - \lambda_2) > 0, \lambda_2(\lambda_1 - \lambda_2) < 0$ and $a^2 - 4bc < 0$ then the orientation of the orbits is reversed. (c) $\lambda_1\lambda_2 > 0, b(\lambda_1 - \lambda_2) < 0, \lambda_2(\lambda_1 - \lambda_2) > 0$ and $a^2 - 4bc < 0$. If $\lambda_1\lambda_2 > 0, b(\lambda_1 - \lambda_2) > 0, \lambda_2(\lambda_1 - \lambda_2) > 0$ and $a^2 - 4bc < 0$ then the orientation of the orbits is reversed.

The eigenvalues of the Jacobian matrix of the vector field defined by system (4) evaluated at (x_0, y_0) are

$$(18) \quad \pm \frac{\sqrt{(a^2 - 4bc)\lambda_1\lambda_2}}{\sqrt{2}}.$$

The eigenvalues of the Jacobian matrix of the vector field defined by system (4) evaluated at (x_j, y_j) are

$$(-1)^{j+1} \frac{|b|\lambda_1\sqrt{a^2 - 4bc}}{b} \quad \text{and} \quad (-1)^{j+1} \frac{|b|\lambda_2\sqrt{a^2 - 4bc}}{b}, \quad j = 1, 2.$$

It follows that (x_j, y_j) is a hyperbolic singular point, for $j = 1, 2$. Moreover, if $\lambda_1\lambda_2 > 0$ then (x_0, y_0) is a hyperbolic singular point and, if $\lambda_1\lambda_2 < 0$ then (x_0, y_0) is a center. Since $(x_j, y_j) \in p \cap l$ for $j = 1, 2$ we obtain that p and l are separatrices of system (4). We present the local phase portrait of system (4) at the singularities (x_0, y_0) , (x_1, y_1) and (x_2, y_2) in Figures 9 and 12.

We will prove that the saddle point is connected with the attracting node and with the repelling node in the cases shown in Figure 12. From this we obtain Figure 8.

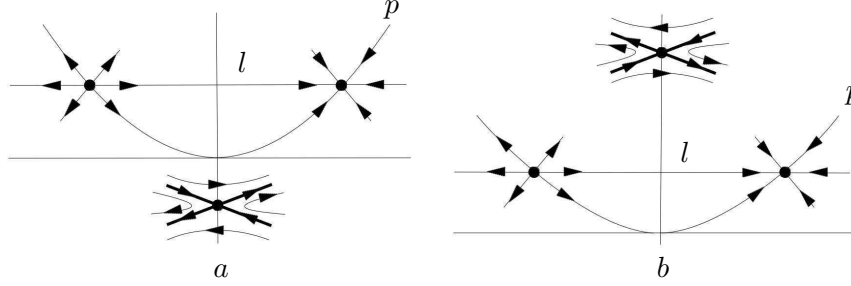
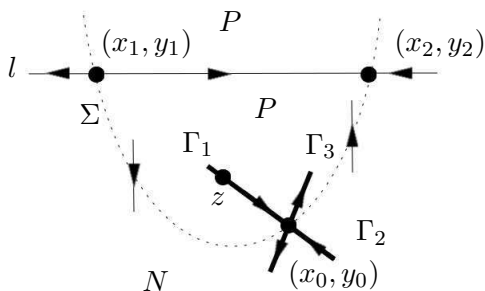


FIGURE 12. Local phase portrait of system (4) with $\lambda_1\lambda_2 \neq 0$, $\lambda_1 \neq \lambda_2$, $b \neq 0$ and $a^2 - 4bc > 0$. (a) $\lambda_1 > \lambda_2 > 0$ and $b > 0$ or $\lambda_1 < \lambda_2 < 0$ and $b < 0$. If $\lambda_1 < \lambda_2 < 0$ and $b > 0$ or $0 < \lambda_2 < \lambda_1$ and $b < 0$ then the orientation of the orbits is reversed. (b) $0 < \lambda_1 < \lambda_2$ and $b > 0$ or $\lambda_2 < \lambda_1 < 0$ and $b < 0$. If $\lambda_2 < \lambda_1 < 0$ and $b > 0$ or $0 < \lambda_1 < \lambda_2$ and $b < 0$ then the orientation of the orbits is reversed.

We consider only the case given by Figure 12-a, because the case given by Figure 12-b follows in a similar way. The portion of Figure 12-a which corresponds to the region below to l is shown in Figure 13. We will prove that $\alpha(\Gamma_1) = \{(x_1, y_1)\}$. It is sufficient to prove that $\Gamma_1 \subset P$. The proof of $\alpha(\Gamma_3) = \{(x_2, y_2)\}$ is analogous.

In Figure 13 we suppose that $a/b \leq 0$. The case $a/b > 0$ is treated in a similar way.

Under the hypotheses of Lemma 16 we obtain that Σ is given by the points of the parabola $b(\lambda_1 - \lambda_2)y = b\lambda_1x^2 + a\lambda_2x + c\lambda_2$ and it is represented as the dashed line in Figure 13. Observe that $(x_j, y_j) \in \Sigma$, $j = 0, 1, 2$ and $x_1 < x_0 < x_2$. Since P and N are connected subsets of \mathbb{R}^2 we obtain that the sets $\Gamma \cap P$ and $\Gamma \cap N$ are also connected, for all orbit Γ of system (4).


 FIGURE 13. Proof of $\alpha(\Gamma_1) = \{(x_1, y_1)\}$.

The slope of the tangent to Σ at (x_0, y_0) is $-a/b$. The slope of the stable subspace of the linearized system at (x_0, y_0) is

$$-\frac{a}{b} - \frac{\sqrt{2}\sqrt{(a^2 - 4bc)\lambda_1\lambda_2}}{2b(\lambda_1 - \lambda_2)},$$

which is smaller than $-a/b$, since $2b(\lambda_1 - \lambda_2) > 0$. From the Stable Manifold Theorem it follows that $\Gamma_1 \cap P \neq \emptyset$ and $\Gamma_2 \cap N \neq \emptyset$.

Since $\dot{y}|_\Sigma$ is given by the polynomial function on the left side of equation (16) divided by $b(\lambda_2 - \lambda_1)$, we have

$$(19) \quad \dot{y}|_\Sigma > 0 \text{ if } x < x_1 \text{ or } x_0 < x < x_2$$

and

$$(20) \quad \dot{y}|_\Sigma < 0 \text{ if } x_1 < x < x_0 \text{ or } x_2 < x.$$

Now we will prove that $\Gamma_1 \subset P$. Suppose that this statement is false. Let $\phi = (\phi_1, \phi_2)$ the flow of the vector field defined by system (4) and take $z \in \Gamma_1 \cap P$. Using continuity it follows that there exists $t_0 \in \mathbb{R}$ such that $\phi(t_0, z) \in \Sigma$. Observe that $\phi(t_0, z) \neq (x_0, y_0)$ because $z \in \Gamma_1$. Then there exist two possibilities: $\phi_1(t_0, z) > x_0$ or $\phi_1(t_0, z) < x_0$.

Suppose that $\phi_1(t_0, z) > x_0$. Since $\dot{\phi}_1(t_0, z) = 0$, from (19) it follows that the solution $\phi(t_0, z)$ is transversal to Σ at $\phi(t_0, z)$. Using the Flow Box Theorem there exist $t_1, t_2 \in \mathbb{R}$ such that $t_1 < t_0 < t_2$ and

$$t_1 \leq t < t_0 \Rightarrow \phi(t, z) \in N \quad \text{and} \quad t_0 < t \leq t_2 \Rightarrow \phi(t, z) \in P.$$

Since $t \mapsto \phi_1(t, z)$ is an increasing function on the interval $(t_0, t_2]$ we have that $\phi_1(t_2, z) > x_0$. But $\lim_{t \rightarrow +\infty} \phi_1(t, z) = x_0$, then there exists $t_3 > t_2$ such that $\dot{\phi}_1(t_3, z) < 0$, that is $\phi(t_3, z) \in N$. Hence we have $t_1 < t_2 < t_3$ with $\phi(t_1, z), \phi(t_3, z) \in N$ and $\phi(t_2, z) \notin N$. This is a contradiction with the fact that the set $\Gamma_1 \cap N$ is connected.

If $\phi_1(t_0, z) < x_0$, using (20) instead (19), we obtain in a similar way a contradiction with the fact that the set $\Gamma_1 \cap P$ is connected.

Case 2: $a^2 = 4bc$. The unique solution of equation (17) is $x = 0$, then the unique singularity (x_0, y_0) of system (4) is given by $x_0 = -a/(2b)$ and $y_0 = c/b$. Observe that $(x_0, y_0) \in p \cap l$. Moreover the tangent line to p at (x_0, y_0) is l .

The Jacobian matrix of the vector field defined by system (4) evaluated at (x_0, y_0) is

$$(\lambda_1 - \lambda_2) \begin{pmatrix} a & b \\ -a^2/b & -a \end{pmatrix}.$$

Then (x_0, y_0) is a nilpotent singularity of system (4).

Doing the translation given by $x \mapsto x - x_0, y \mapsto y - y_0$ system (4) becomes

$$(21) \quad \begin{aligned} \dot{x} &= a(\lambda_1 - \lambda_2)x + b(\lambda_1 - \lambda_2)y - b\lambda_1x^2, \\ \dot{y} &= -4c(\lambda_1 - \lambda_2)x - a(\lambda_1 - \lambda_2)y - a(2\lambda_2 - \lambda_1)x^2 - 2b\lambda_2xy. \end{aligned}$$

After the linear change of coordinates defined by

$$\begin{pmatrix} x \\ y \end{pmatrix} \mapsto \begin{pmatrix} 1/b & 0 \\ a/b^2 & 1/b \end{pmatrix} \begin{pmatrix} x \\ y \end{pmatrix},$$

system (21) becomes

$$(22) \quad \dot{x} = b(\lambda_1 - \lambda_2)y - b^2\lambda_1x^2, \quad y' = -2b^2\lambda_2xy.$$

In order to obtain information on the localization of the separatrices we take the quasi-homogeneous blow-up in the x -direction given by $x = u, y = u^2v$. Then system (22) becomes

$$(23) \quad \dot{u} = b(\lambda_1 - \lambda_2)u^2v - b^2\lambda_1u^2, \quad \dot{v} = -2b(\lambda_1 - \lambda_2)uv^2 + 2b^2(\lambda_1 - \lambda_2)uv.$$

Taking the rescaling given by $ds = u dt$ system (23) writes

$$(24) \quad u' = b(\lambda_1 - \lambda_2)uv - b^2\lambda_1u, \quad v' = -2b(\lambda_1 - \lambda_2)v^2 + 2b^2(\lambda_1 - \lambda_2)v.$$

The singularities (u_0, v_0) of system (24) with $u_0 = 0$ are $(0, 0)$ and $(0, b)$.

The eigenvalues of the Jacobian matrix of the vector field defined by system (24) evaluated at $(0, 0)$ and $(0, b)$ are $-b^2\lambda_1, 2b^2(\lambda_1 - \lambda_2)$ and $-b^2, -2b^2(\lambda_1 - \lambda_2)$, respectively.

Changing y by $-y$ and v by $-v$, Figure 14 corresponds also to the case $b < 0$ and $\lambda_1 < \lambda_2 < 0$. If $b < 0$ and $0 < \lambda_2 < \lambda_1$ then the orientation of the orbits is reversed.

Changing y by $-y$ and v by $-v$, Figure 15 corresponds also to the case $b < 0$ and $\lambda_2 < \lambda_1 < 0$. If $b < 0$ and $0 < \lambda_1 < \lambda_2$ then the orientation of the orbits is reversed.

Changing y by $-y$ and v by $-v$, Figure 16 corresponds also to the case $b < 0$ and $\lambda_1 < 0 < \lambda_2$. If $b < 0$ and $\lambda_2 < 0 < \lambda_1$ then the orientation of the orbits is reversed.

Observe that for system (22) we have $\dot{x}|_{x=0} = b(\lambda_1 - \lambda_2)y$. System (22) is invariant under the change of coordinates $(t, x, y) \mapsto (-t, -x, y)$, then system (22) is symmetric with respect to the y -axis. Then we obtain the following conclusions. If $\lambda_1\lambda_2 > 0$ then the sectorial decomposition of system (22) at $(0, 0)$ is composed by one elliptic sector, one hyperbolic sector, one attracting sector and one repelling sector. If $\lambda_1\lambda_2 < 0$ then $(0, 0)$ is a saddle point of system (22).

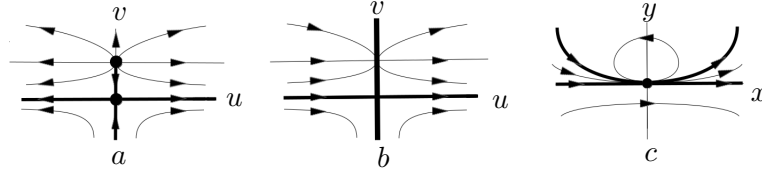


FIGURE 14. Local phase portrait of system (22) at $(0, 0)$ for the case $b > 0$ and $\lambda_1 < \lambda_2 < 0$. If $b > 0$ and $0 < \lambda_2 < \lambda_1$ then the orientation of the orbits is reversed. (a) System (24). (b) System (23). (c) System (22).

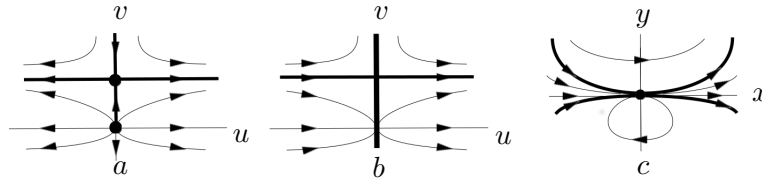


FIGURE 15. Local phase portrait of system (22) at $(0, 0)$ for the case $b > 0$ and $\lambda_2 < \lambda_1 < 0$. If $b > 0$ and $0 < \lambda_1 < \lambda_2$ then the orientation of the orbits is reversed. (a) System (24). (b) System (23). (c) System (22).

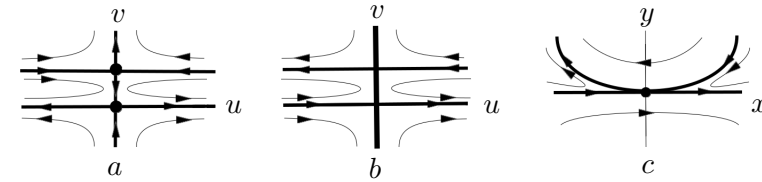


FIGURE 16. Local phase portrait of system (22) at $(0, 0)$ for the case $b > 0$ and $\lambda_1 < 0 < \lambda_2$. If $b > 0$ and $\lambda_2 < 0 < \lambda_1$ then the orientation of the orbits is reversed. (a) System (24). (b) System (23). (c) System (22).

Observe that from the blow-up we obtain that the straight line $v = b$ of system (24) corresponds to the parabola $y = bx^2$ of system (22). Then we have the following conclusions on the separatrices of system (22). For the cases of Figure 14 the separatrices are contained in the axis $y = 0$ and in the region $y \geq bx^2$. For the cases of Figure 15 the separatrices are contained in

$y = bx^2$ and in the region $y \leq 0$. For the cases of Figure 16 the separatrices are contained in $y = bx^2$ and in $y = 0$.

We present the sectorial decomposition of system (4) at (x_0, y_0) in the Figure 10.

Case 3: $a^2 < 4bc$. In this case the unique solution of equation (17) is $x = 0$, then the unique singularity (x_0, y_0) of system (4) is given by $x_0 = -a/(2b)$ and $y_0 = ((4bc - a^2)\lambda_2 + a^2(\lambda_1 - \lambda_2))/(4b^2(\lambda_1 - \lambda_2))$. Observe that $(x_0, y_0) \notin p \cup l$.

The eigenvalues of the Jacobian matrix of the vector field defined by system (4) evaluated at (x_0, y_0) are given by (18). If $\lambda_1\lambda_2 < 0$ then (x_0, y_0) is a hyperbolic saddle point of system (4). If $\lambda_1\lambda_2 > 0$ then the eigenvalues are purely imaginary and (x_0, y_0) is a center of system (4). We show the sectorial decomposition of system (4) at (x_0, y_0) in Figure 11. The proof of statement (a) is complete.

The proof of statement (b) is analogous to the proof of $\alpha(\Gamma_1) = \{(x_1, y_1)\}$ done in Case 2. \square

5.2. Infinite singularities of system (4). The expression of the Poincaré compactification of system (4) in the charts (U_1, φ_1) and (U_2, φ_2) is

$$(25) \quad \begin{aligned} \dot{u} &= \lambda_2(a + bu + cv)(uv - 2) + \lambda_1(1 - uv)(a + bu), \\ \dot{v} &= \lambda_2(a + bu + cv)v^2 + b\lambda_1(1 - uv)v, \end{aligned}$$

and

$$(26) \quad \begin{aligned} \dot{u} &= \lambda_2(au + b + cv)(2u^2 - v) + \lambda_1(v - u^2)(au + b), \\ \dot{v} &= 2\lambda_2(au + b + cv)uv + a\lambda_1(v - u^2)v, \end{aligned}$$

respectively.

5.2.1. Infinite singularities in U_1 . In this section we will determine the sectorial decomposition of the singularities of system (25) which are of the form $(u, 0)$, with $u \in \mathbb{R}$. We consider the cases $\lambda_1 - 2\lambda_2 \neq 0$ and $\lambda_1 - 2\lambda_2 = 0$ separately. The first one, studied in Lemma 11, follows from the Grobman-Hartman Theorem and the proof is omitted. In the second case $v = 0$ is a line of singularities and we study the phase portrait of the corresponding system in Lemma 12.

Lemma 11. *Suppose that $\lambda_1\lambda_2 \neq 0$ and $\lambda_1 - 2\lambda_2 \neq 0$.*

- (a) *If $b = 0$ then system (25) has no singularities in a neighborhood of the axis $v = 0$.*
- (b) *Suppose $b \neq 0$. Then the unique singularity (u_0, v_0) of system (25) with $v_0 = 0$ is given by $u_0 = -a/b$. If $b\lambda_1 > 0$ and $b(\lambda_1 - 2\lambda_2) > 0$ then $(u_0, 0)$ is a hyperbolic repelling node of system (25). If $b\lambda_1 < 0$ and $b(\lambda_1 - 2\lambda_2) < 0$ then $(u_0, 0)$ is a hyperbolic attracting node of*

system (25). If $\lambda_1(\lambda_1 - 2\lambda_2) < 0$ then $(u_0, 0)$ is a hyperbolic saddle point of system (25).

Lemma 12. Suppose that $\lambda_1\lambda_2 \neq 0$ and $\lambda_1 - 2\lambda_2 = 0$. The phase portrait of system (25) in \mathbb{R}^2 is shown in Figure 17.

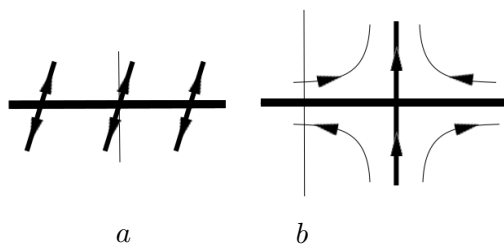


FIGURE 17. Phase portrait of system (25). (a) $\lambda_1 = 2\lambda_2$ and $b\lambda_2 > 0$. If $\lambda_1 = 2\lambda_2$ and $b\lambda_2 < 0$ then the orientation of the orbits is reversed. (b) $\lambda_1 = 2\lambda_2, b = 0$ and $a\lambda_2 > 0$. If $\lambda_1 = 2\lambda_2, b = 0$ and $a\lambda_2 < 0$ then the orientation of the orbits is reversed.

Proof. After the rescaling given by $ds = \lambda_2 v dt$ system (25) becomes

$$(27) \quad u' = cuv - bu^2 - au - 2c, \quad v' = cv^2 + (a - bu)v + 2b.$$

We consider the cases $b \neq 0$ and $b = 0$ separately.

Case 1: $b \neq 0$. In this case system (27) has no singularities (u_0, v_0) with $v_0 = 0$ and we show the phase portrait of system (25) in a sufficiently small neighborhood of the axis $v = 0$ in Figure 17-a.

Case 2: $b = 0$. From hypothesis $a^2 + b^2 \neq 0$ it follows that $a \neq 0$. In this case the unique singularity (u_0, v_0) of system (27) with $v_0 = 0$ is $u_0 = -2c/a$.

The eigenvalues of the Jacobian matrix of the vector field defined by system (27) evaluated at $(u_0, 0)$ are $-a$ and $-2c^2/a$. Then $(u_0, 0)$ is a hyperbolic saddle point of system (27). We present the phase portrait of system (25) in a sufficiently small neighborhood of the axis $v = 0$ in Figure 17-b. \square

5.2.2. *The origin of U_2 .* We denote by p' the parabola given by $v = u^2$. From Remark 5 it follows that the points of $p \setminus \{(0, 0)\}$ are mapped into the points of p' .

The Jacobian matrix of the vector field defined by system (26) evaluated at $(0, 0)$ is

$$\begin{pmatrix} 0 & b(\lambda_1 - \lambda_2) \\ 0 & 0 \end{pmatrix}.$$

Then we consider the cases $b = 0$, $b \neq 0$ and $\lambda_1 = \lambda_2$, and $b(\lambda_1 - \lambda_2) \neq 0$ separately. In the last case the origin is a nilpotent singularity of system

(26). In order to obtain information on the localization of the separatrices we will use blow-ups to study the singularity $(0, 0)$.

Lemma 13. *Suppose that $\lambda_1\lambda_2 \neq 0$ and $b = 0$.*

- (a) *If $\lambda_1 \neq 2\lambda_2$ then the sectorial decomposition of system (26) at the origin is shown in Figure 18.*
 (b) *If $\lambda_1 = 2\lambda_2$ then the sectorial decomposition of system (26) at the origin is shown in Figure 19.*

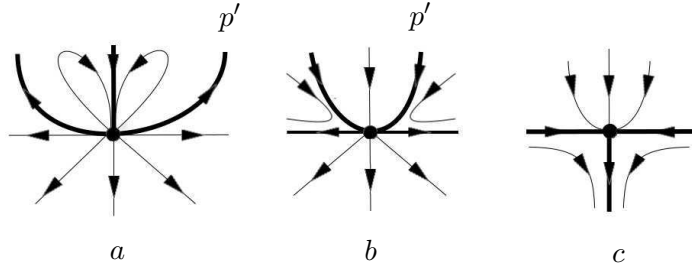


FIGURE 18. Sectorial decomposition of system (26) at $(0, 0)$ for the case $b = 0$. (a) $a\lambda_1 < 0, a\lambda_2 > 0$ and $a(\lambda_1 - 2\lambda_2) < 0$. If $a\lambda_1 > 0, a\lambda_2 < 0$ and $a(\lambda_1 - 2\lambda_2) > 0$ then the orientation of the orbits is reversed. (b) $a\lambda_1 < 0, a\lambda_2 < 0$ and $a(\lambda_1 - 2\lambda_2) < 0$. If $a\lambda_1 > 0, a\lambda_2 > 0$ and $a(\lambda_1 - 2\lambda_2) > 0$ then the orientation of the orbits is reversed. (c) $a\lambda_1 < 0, a\lambda_2 < 0$ and $a(\lambda_1 - 2\lambda_2) > 0$. If $a\lambda_1 > 0, a\lambda_2 > 0$ and $a(\lambda_1 - 2\lambda_2) < 0$ then the orientation of the orbits is reversed.

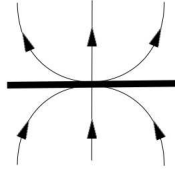


FIGURE 19. Sectorial decomposition of system (26) at $(0, 0)$ for the case $\lambda_1\lambda_2 \neq 0, b = 0, \lambda_1 = 2\lambda_2$ and $a\lambda_2 > 0$. If $\lambda_1\lambda_2 \neq 0, b = 0, \lambda_1 = 2\lambda_2$ and $a\lambda_2 < 0$ then the orientation of the orbits is reversed.

Proof. We consider the cases $\lambda_1 - 2\lambda_2 \neq 0$ and $\lambda_1 - 2\lambda_2 = 0$ separately.

Case 1: $\lambda_1 - 2\lambda_2 \neq 0$. We take the quasi-homogeneous blow-up in the positive v -direction given by $u = \bar{u} \bar{v}, v = \bar{v}^2$. Then system (26) becomes

$$(28) \quad \begin{aligned} \dot{\bar{u}} &= \frac{1}{2} [2c\lambda_2(\bar{u}^2 - 1)\bar{v}^3 + a(2\lambda_2 - \lambda_1)(\bar{u}^2 - 1)\bar{u} \bar{v}^2], \\ \dot{\bar{v}} &= \frac{1}{2} [c\lambda_2\bar{u} \bar{v} + ((2\lambda_2 - \lambda_1)\bar{u}^2 + a\lambda_1)] \bar{v}^3. \end{aligned}$$

Taking the rescaling **given by** $ds = \bar{v}^2/2 dt$ **system** (28) becomes

$$(29) \quad \begin{aligned} \bar{u}' &= c\lambda_2(\bar{u}^2 - 1)\bar{v} + a(2\lambda_2 - \lambda_1)(\bar{u}^2 - 1)\bar{u}, \\ \bar{v}' &= [c\lambda_2\bar{u}\bar{v} + (a(2\lambda_2 - \lambda_1)\bar{u}^2 + a\lambda_1)]\bar{v}. \end{aligned}$$

The singularities (\bar{u}_0, \bar{v}_0) of system (29) with $\bar{v}_0 = 0$ are $(0, 0)$ and $(\pm 1, 0)$. **The eigenvalues of the Jacobian matrix of the vector field defined by system (29) evaluated at $(0, 0)$ are $-a(2\lambda_2 - \lambda_1)$ and $a\lambda_1$. The eigenvalues of the Jacobian matrix of the vector field defined by system (29) evaluated at $(1, 0)$ or $(-1, 0)$ are $2a(2\lambda_2 - \lambda_1)$ and $2a\lambda_2$.** Then $(0, 0)$ and $(\pm 1, 0)$ are hyperbolic singularities of system (29).

For system (26) we have that

$$(30) \quad \dot{u}|_{v=0} = a(2\lambda_2 - \lambda_1)u^3 \quad \text{and} \quad \dot{v}|_{u=0} = a\lambda_1 v^2.$$

Observe that the straight lines $\bar{u} = \pm 1$ are invariant under the flow of the system (29), then the parabola p' **contain separatrices** of system (26) for the cases present in Figures 20 and 21. The quasi-homogeneous blow-up in the positive v -direction is summarized in Figures 20-22.

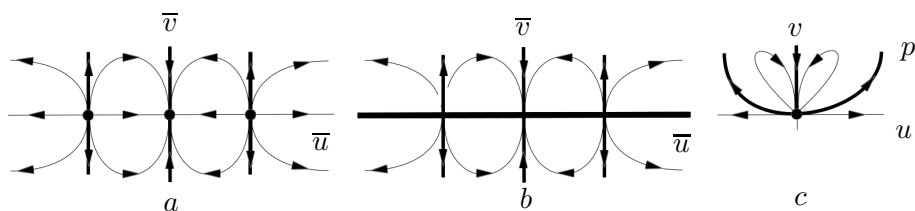


FIGURE 20. Sectorial decomposition of system (26) at $(0, 0)$ with $v \geq 0$, for the case $b = 0, a(2\lambda_2 - \lambda_1) > 0, a\lambda_2 > 0$ and $a\lambda_1 < 0$. If $b = 0, a(2\lambda_2 - \lambda_1) < 0, a\lambda_2 < 0$ and $a\lambda_1 > 0$ then the orientation of the orbits is reversed. (a) System (29). (b) System (28). (c) Sectorial decomposition of system (26) at $(0, 0)$ with $v \geq 0$.

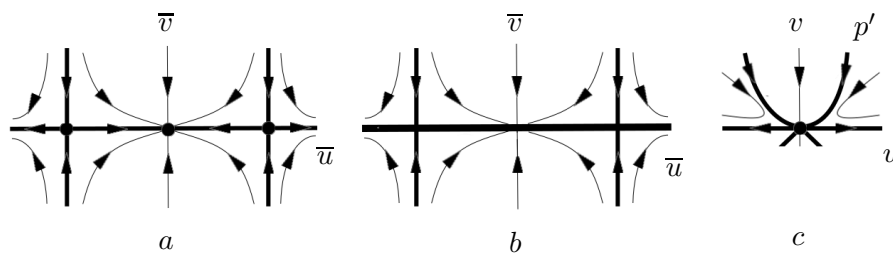


FIGURE 21. Sectorial decomposition of system (26) at $(0, 0)$ with $v \geq 0$, for the case $b = 0, a(2\lambda_2 - \lambda_1) > 0, a\lambda_2 < 0$ and $a\lambda_1 < 0$. If $b = 0, a(2\lambda_2 - \lambda_1) < 0, a\lambda_2 > 0$ and $a\lambda_1 > 0$ then the orientation of the orbits is reversed. (a) System (29). (b) System (28). (c) Sectorial decomposition of system (26) at $(0, 0)$ with $v \geq 0$.

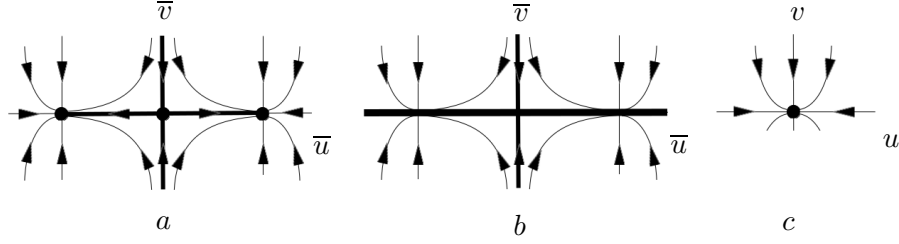


FIGURE 22. Sectorial decomposition of system (26) at $(0, 0)$ with $v \geq 0$, for the case $b = 0, a(2\lambda_2 - \lambda_1) < 0, a\lambda_2 < 0$ and $a\lambda_1 < 0$. If $b = 0, a(2\lambda_2 - \lambda_1) > 0, a\lambda_2 > 0$ and $a\lambda_1 > 0$ then the orientation of the orbits is reversed. (a) System (29). (b) System (28). (c) Sectorial decomposition of system (26) at $(0, 0)$ with $v \geq 0$.

We take the quasi-homogeneous blow-up in the negative v -direction given by $u = \bar{u} \bar{v}$, $v = -\bar{v}^2$. Then system (26) becomes

$$\begin{aligned} \dot{\bar{u}} &= -\frac{1}{2} [2c\lambda_2(\bar{u}^2 + 1)\bar{v} + a(\lambda_1 - 2\lambda_2)(\bar{u}^3 + \bar{u})] \bar{v}^2, \\ \dot{\bar{v}} &= -\frac{1}{2} [2c\lambda_2\bar{u}\bar{v} + a((\lambda_1 - 2\lambda_2)\bar{u}^2 + \lambda_1)] \bar{v}^3. \end{aligned} \quad (31)$$

Observe that this change of coordinates maps points (\bar{u}, \bar{v}) with $\bar{v} > 0$ in points (u, v) with $v < 0$. Taking the rescaling given by $ds = \bar{v}^2/2 dt$ system (31) becomes

$$\begin{aligned} \bar{u}' &= - [2c\lambda_2(\bar{u}^2 + 1)\bar{v} + a(\lambda_1 - 2\lambda_2)(\bar{u}^3 + \bar{u})], \\ \bar{v}' &= - [2c\lambda_2\bar{u}\bar{v} + a((\lambda_1 - 2\lambda_2)\bar{u}^2 + \lambda_1)] \bar{v}. \end{aligned} \quad (32)$$

The singularity (\bar{u}_0, \bar{v}_0) of system (32) with $\bar{v}_0 = 0$ is $(0, 0)$. **The eigenvalues of the Jacobian matrix of the vector field defined by system (32) evaluated at $(0, 0)$ are $a(2\lambda_2 - \lambda_1)$ and $-a\lambda_1$.** Then $(0, 0)$ is a hyperbolic singular point of system (32).

Using (30) we summarize the quasi-homogeneous blow-up in the negative v -direction in Figures 23 and 24.

The sectorial decomposition of system (26) at $(0, 0)$ shown in Figure 18-a follows from Figure 20-c and Figure 24-c (with reversed orientation). The sectorial decomposition of system (26) at $(0, 0)$ given in Figure 18-b follows from Figure 21-c and Figure 24-c (with reversed orientation). The sectorial decomposition of system (26) at $(0, 0)$ shown in Figure 18-c follows from Figure 22-c and Figure 23-c (with reversed orientation).

Case 2: $\lambda_1 = 2\lambda_2$. After the rescaling given by $ds = \lambda_2 v dt$ system (26) becomes

$$u' = -cv + 2cu^2 + au, \quad v' = 2(cu + a)v. \quad (33)$$

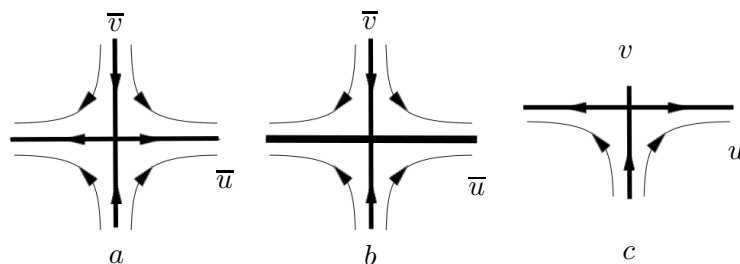


FIGURE 23. Sectorial decomposition of system (26) at $(0,0)$ with $v \leq 0$, for the case $\lambda_2 \neq 0, b = 0, a\lambda_1 > 0$ and $a(2\lambda_2 - \lambda_1) > 0$. If $\lambda_2 \neq 0, b = 0, a\lambda_1 < 0$ and $a(2\lambda_2 - \lambda_1) < 0$ then the orientation of the orbits is reversed. (a) System (32). (b) System (31). (c) Sectorial decomposition of system (26) at $(0,0)$ with $v \leq 0$.

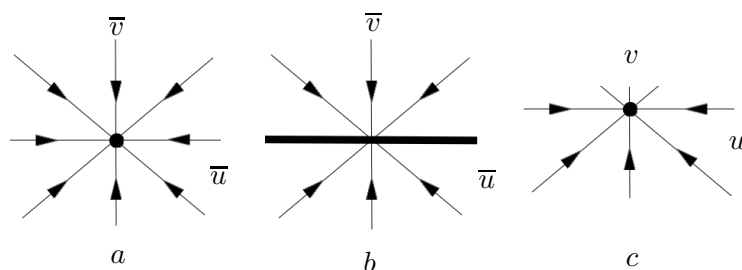


FIGURE 24. Sectorial decomposition of system (26) at $(0,0)$ with $v \leq 0$, for the case $\lambda_2 \neq 0, b = 0, a\lambda_1 > 0$ and $a(2\lambda_2 - \lambda_1) < 0$. If $\lambda_2 \neq 0, b = 0, a\lambda_1 < 0$ and $a(2\lambda_2 - \lambda_1) > 0$ then the orientation of the orbits is reversed. (a) System (32). (b) System (31). (c) Sectorial decomposition of system (26) at $(0,0)$ with $v \leq 0$.

The eigenvalues of the Jacobian matrix of the vector field defined by system (33) evaluated at $(0,0)$ are a and $2a$. Then $(0,0)$ is a hyperbolic singular point of system (33). We present the local phase portrait of system (26) at $(0,0)$ in Figure 19. \square

Observe that in Lemma 14-e, we will present a finite number of possibilities for the sectorial decomposition of system (26). But in the proof of Theorem 1 we will prove that the sectorial decomposition of system (26) at the origin, for this case, is composed by two elliptic sectors.

Lemma 14. *Suppose that $\lambda_1\lambda_2 \neq 0, b \neq 0$ and $\lambda_1 = \lambda_2$.*

- (a) *If $a = c = 0$ then the sectorial decomposition of system (26) at the origin is shown in Figure 30.*
- (b) *If $c = 0$ and $a \neq 0$ then the sectorial decomposition of system (26) at the origin is given in Figures 25-c and 26-c.*

- (c) If $c \neq 0$ and $a^2 > 4bc$ then the sectorial decomposition of system (26) at the origin is shown in Figures 27-c, 28-c and 29-c.
- (d) If $c \neq 0$ and $a^2 = 4bc$ then the sectorial decomposition of system (26) at the origin is shown in Figures 31-d and 32-d.
- (e) If $c \neq 0$ and $a^2 < 4bc$ then the sectorial decomposition of system (26) at the origin is given in Figure 33-c.

Proof. Taking the rescaling given by $ds = \lambda_1 dt$ system (26) becomes

$$(34) \quad u' = 2cu^2v + au^3 - cv^2 + bu^2, \quad v' = 2cv^2 + au^2v + av^2 + 2buv.$$

We take the blow-up in the u -direction given by $u = \bar{u}$, $v = \bar{u}\bar{v}$, which maps points of the form $u < 0$, $v > 0$ into points of the form $\bar{u} < 0$, $\bar{v} < 0$; and points of the form $u < 0$, $v < 0$ into points of the form $\bar{u} < 0$, $\bar{v} > 0$. Then system (34) becomes

$$(35) \quad \dot{\bar{u}} = -c\bar{u}^2\bar{v}^2 + 2c\bar{u}^3\bar{v} + a\bar{u}^3 + b\bar{u}^2, \quad \dot{\bar{v}} = c\bar{u}\bar{v}^3 + a\bar{u}\bar{v}^2 + b\bar{u}\bar{v}.$$

Taking the rescaling given by $ds = \bar{u} dt$ system (35) becomes

$$(36) \quad \bar{u}' = -c\bar{u}\bar{v}^2 + 2c\bar{u}^2\bar{v} + a\bar{u}^2 + b\bar{u}, \quad \bar{v}' = c\bar{v}^3 + a\bar{v}^2 + b\bar{v}.$$

The singularities (\bar{u}_0, \bar{v}_0) of system (36) with $\bar{u}_0 = 0$ are $(0, 0)$ and $(0, \bar{v}_0)$, where \bar{v}_0 is a solution of the equation $c\bar{v}^2 + a\bar{v} + b = 0$. **The eigenvalues of the Jacobian matrix of the vector field defined by system (36) evaluated at $(0, 0)$ are equal to b , then $(0, 0)$ is a hyperbolic singular point of system (36).** In order to study the other singularities of system (36) we consider three cases.

Case 1: $a^2 - 4bc > 0$.

Case 1.1: $c = 0$. Then $a \neq 0$. The singularities (\bar{u}_0, \bar{v}_0) of system (36) with $\bar{u} = 0$ are $(0, 0)$ and $(0, -b/a)$. **The eigenvalues of the Jacobian matrix of the vector field defined by system (36) evaluated at $(0, -b/a)$ are b and $-b$.** Observe that the straight line $\bar{v} = -b/a$ is invariant for system (36), then the straight line $v = -(b/a)u$ is invariant for system (26). **Moreover, since $\lambda_1 = \lambda_2$ and $c = 0$, the axis $u = 0$ is invariant for system (26).** We summarize the blow-up in Figures 25 and 26.

Case 1.2: $c \neq 0$. The singularities (\bar{u}_0, \bar{v}_0) of system (36) with $\bar{u} = 0$ are $(0, 0)$, $(0, \bar{v}_1)$ and $(0, \bar{v}_2)$, where $\bar{v}_1 = (-a + \sqrt{a^2 - 4bc})/(2c)$ and $\bar{v}_2 = -(a + \sqrt{a^2 - 4bc})/(2c)$. **The eigenvalues of the Jacobian matrix of the vector field defined by system (36) evaluated at $(0, \bar{v}_j)$ are $\pm \bar{v}_j \sqrt{a^2 - 4bc}$, for $j = 1, 2$.** Observe that the straight line $\bar{v} = \bar{v}_j$ is invariant for system (36), then the straight line $v = \bar{v}_j u$ are invariant for system (26), for $j = 1, 2$. The blow-up is summarized in Figures 27-29.

Case 2: $a^2 = 4bc$.

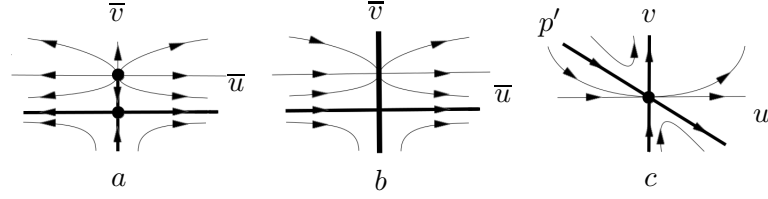


FIGURE 25. Sectorial decomposition of system (26) at $(0,0)$ for the case $\lambda_1 = \lambda_2 > 0, a > 0, b > 0$ and $c = 0$; or $\lambda_1 = \lambda_2 < 0, a < 0, b < 0$ and $c = 0$. If $\lambda_1 = \lambda_2 > 0, a < 0, b < 0$ and $c = 0$; or $\lambda_1 = \lambda_2 < 0, a > 0, b > 0$ and $c = 0$ then the orientation of the orbits is reversed. (a) System (36). (b) System (35). (c) Sectorial decomposition of system (26) at $(0,0)$.

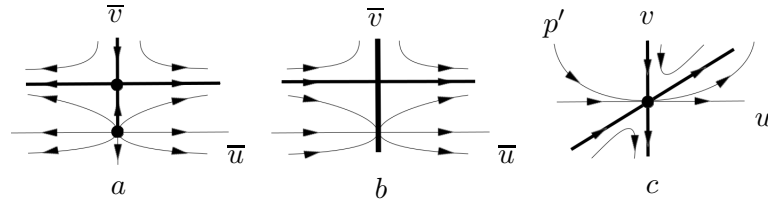


FIGURE 26. Sectorial decomposition of system (26) at $(0,0)$ for the case $\lambda_1 = \lambda_2 > 0, a < 0, b > 0$ and $c = 0$; or $\lambda_1 = \lambda_2 < 0, a > 0, b < 0$ and $c = 0$. If $\lambda_1 = \lambda_2 < 0, a < 0, b > 0$ and $c = 0$; or $\lambda_1 = \lambda_2 > 0, a > 0, b < 0$ and $c = 0$ then the orientation of the orbits is reversed. (a) System (36). (b) System (35). (c) Sectorial decomposition of system (26) at $(0,0)$.

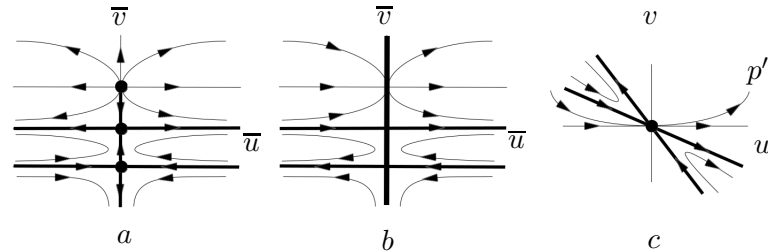


FIGURE 27. Sectorial decomposition of system (26) at $(0,0)$ for the case $\lambda_1 = \lambda_2 > 0, a > 0, b > 0, c > 0$ and $a^2 - 4bc > 0$; or $\lambda_1 = \lambda_2 < 0, a < 0, b < 0, c < 0$ and $a^2 - 4bc > 0$. If $\lambda_1 = \lambda_2 < 0, a > 0, b > 0, c > 0$ and $a^2 - 4bc > 0$; or $\lambda_1 = \lambda_2 > 0, a < 0, b < 0, c < 0$ and $a^2 - 4bc > 0$ then the orientation of the orbits is reversed. (a) System (36). (b) System (35). (c) Sectorial decomposition of system (26) at $(0,0)$.

Case 2.1: $a = c = 0$. In this case the blow-up is superfluous. Taking the rescaling given by $ds = u dt$ in system (34), we obtain the sectorial decomposition of system (26) at $(0,0)$ shown in Figure 30.

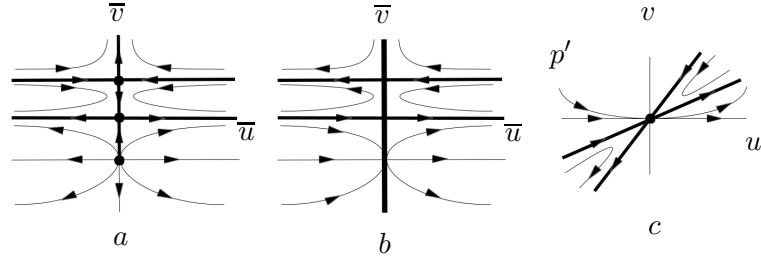


FIGURE 28. Sectorial decomposition of system (26) at $(0,0)$ for the case $\lambda_1 = \lambda_2 > 0, a < 0, b > 0, c > 0$ and $a^2 - 4bc > 0$; or $\lambda_1 = \lambda_2 < 0, a > 0, b < 0, c < 0$ and $a^2 - 4bc > 0$. If $\lambda_1 = \lambda_2 < 0, a < 0, b > 0, c > 0$ and $a^2 - 4bc > 0$; or $\lambda_1 = \lambda_2 > 0, a > 0, b < 0, c < 0$ and $a^2 - 4bc > 0$ then the orientation of the orbits is reversed. (a) System (36). (b) System (35). (c) Sectorial decomposition of system (26) at $(0,0)$.

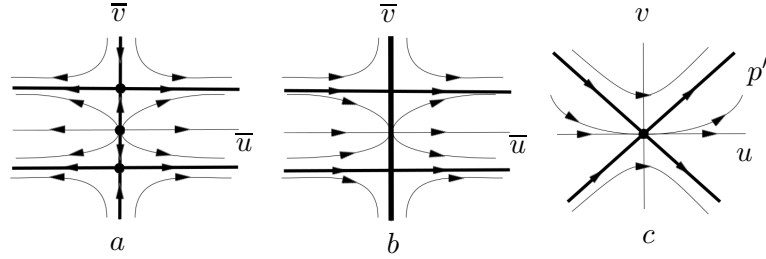


FIGURE 29. Sectorial decomposition of system (26) at $(0,0)$ for the case $\lambda_1 = \lambda_2 > 0, b > 0, c < 0$ and $a^2 - 4bc > 0$; or $\lambda_1 = \lambda_2 < 0, b < 0, c > 0$ and $a^2 - 4bc > 0$. If $\lambda_1 = \lambda_2 < 0, b > 0, c < 0$ and $a^2 - 4bc > 0$; or $\lambda_1 = \lambda_2 > 0, b < 0, c > 0$ and $a^2 - 4bc > 0$ then the orientation of the orbits is reversed. (a) System (36). (b) System (35). (c) Sectorial decomposition of system (26) at $(0,0)$.

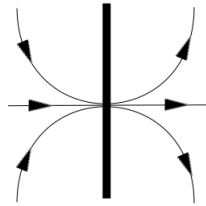


FIGURE 30. Sectorial decomposition of system (26) at $(0,0)$ for the case $\lambda_1 = \lambda_2 \neq 0, a = c = 0$ and $b\lambda_1 > 0$. If $\lambda_1 = \lambda_2 \neq 0, a = c = 0$ and $b\lambda_1 < 0$ then the orientation of the orbits is reversed.

Case 2.2: $ac \neq 0$. The singularities (\bar{u}_0, \bar{v}_0) of system (36) with $\bar{u}_0 = 0$ are $(0,0)$ and $(0, \bar{v}_1)$, where $\bar{v}_1 = -a/(2c)$. Taking the rescaling given by

$d\tau = (\bar{v} - \bar{v}_1) ds$ system (36) becomes

$$(37) \quad \frac{d\bar{u}}{d\tau} = -c\bar{u}\bar{v} + 2c\bar{u}^2 + \frac{a\bar{u}}{2}, \quad \frac{d\bar{v}}{d\tau} = c\bar{v}(\bar{v} - \bar{v}_1).$$

The eigenvalues of the Jacobian matrix of the vector field defined by system (37) evaluated at $(0, 0)$ are equal to $a/2$. The eigenvalues of the Jacobian matrix of the vector field defined by system (37) evaluated at $(0, \bar{v}_1)$ are a and $-a/2$. Since $\lambda_1 = \lambda_2$, for system (26) we observe that $\dot{u}|_{u=0} = -\lambda_1 cv^2$, $\dot{u}|_{v=0} = \lambda_1 u^2(au + b)$ and $\dot{v}|_{u=0} = \lambda_1 av^2$. The blow-up is summarized in Figures 31 and 32.

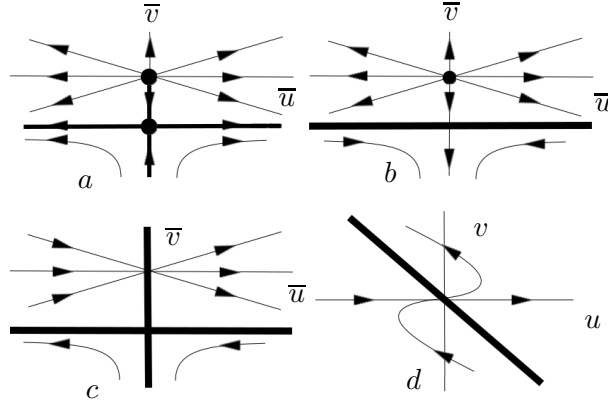


FIGURE 31. Sectorial decomposition of system (26) at $(0, 0)$ for the case $\lambda_1 = \lambda_2 > 0, a > 0, b > 0, c > 0$ and $a^2 - 4bc = 0$; or $\lambda_1 = \lambda_2 < 0, a < 0, b < 0, c < 0$ and $a^2 - 4bc = 0$. If $\lambda_1 = \lambda_2 < 0, a > 0, b > 0, c > 0$ and $a^2 - 4bc = 0$; or $\lambda_1 = \lambda_2 > 0, a < 0, b < 0, c < 0$ and $a^2 - 4bc = 0$ then the orientation of the orbits is reversed. (a) System (37). (b) System (36). (c) System (35). (d) Sectorial decomposition of system (26) at $(0, 0)$.

Case 3. $a^2 < 4bc$. The unique singularity (\bar{u}_0, \bar{v}_0) of system (36) with $\bar{u}_0 = 0$ is $(0, 0)$. The blow-up is summarized in Figure 33. \square

Lemma 15. Suppose that $\lambda_1\lambda_2 \neq 0$ and $b(\lambda_1 - \lambda_2) \neq 0$.

- (a) If $\lambda_1 \neq 2\lambda_2$ then the sectorial decomposition of system (26) at the origin is given in Figure 34.
- (b) If $\lambda_1 = 2\lambda_2$ then the sectorial decomposition of system (26) at the origin is shown in Figure 35.

Proof. We consider the cases $\lambda_1 \neq 2\lambda_2$ and $\lambda_1 = 2\lambda_2$ separately.

Case 1: $\lambda_1 \neq 2\lambda_2$. In order to obtain information on the localization of the separatrices of the sectorial decomposition of system (26) at $(0, 0)$, we

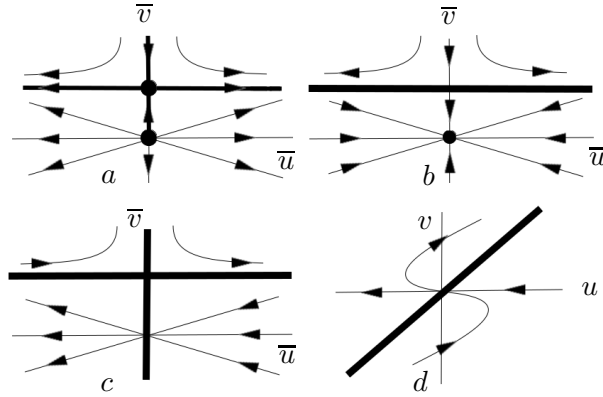


FIGURE 32. Sectorial decomposition of system (26) at $(0, 0)$ for the case $\lambda_1 = \lambda_2 > 0, a > 0, b < 0, c < 0$ and $a^2 - 4bc = 0$; or $\lambda_1 = \lambda_2 < 0, a < 0, b > 0, c > 0$ and $a^2 - 4bc = 0$. If $\lambda_1 = \lambda_2 > 0, a < 0, b > 0, c > 0$ and $a^2 - 4bc = 0$; or $\lambda_1 = \lambda_2 < 0, a > 0, b < 0, c < 0$ and $a^2 - 4bc = 0$ then the orientation of the orbits is reversed. (a) System (37). (b) System (36). (c) System (35). (d) Sectorial decomposition of system (26) at $(0, 0)$.

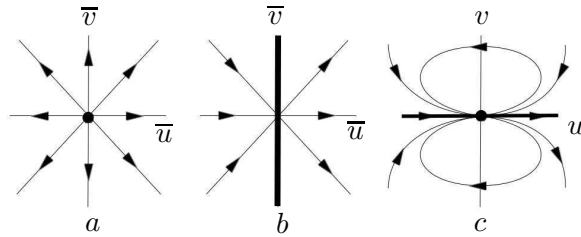


FIGURE 33. Sectorial decomposition of system (26) at $(0, 0)$ for the case $\lambda_1 = \lambda_2 > 0, b > 0, c > 0$ and $a^2 - 4bc < 0$; or $\lambda_1 = \lambda_2 < 0, b < 0, c < 0$ and $a^2 - 4bc < 0$. If $\lambda_1 = \lambda_2 < 0, b > 0, c > 0$ and $a^2 - 4bc < 0$; or $\lambda_1 = \lambda_2 > 0, b < 0, c < 0$ and $a^2 - 4bc < 0$ then the orientation of the orbits is reversed. (a) System (36). (b) System (35). (c) Sectorial decomposition of system (26) at $(0, 0)$.

will use blow-up. Moreover, if we use Theorem 3.5 of [7], then the case $\lambda_1 = 3\lambda_2$ should be treated separately.

We take the quasi-homogeneous blow-up in the u -direction given by $u = \bar{u}, v = \bar{u}^2 \bar{v}$. Then system (26) becomes

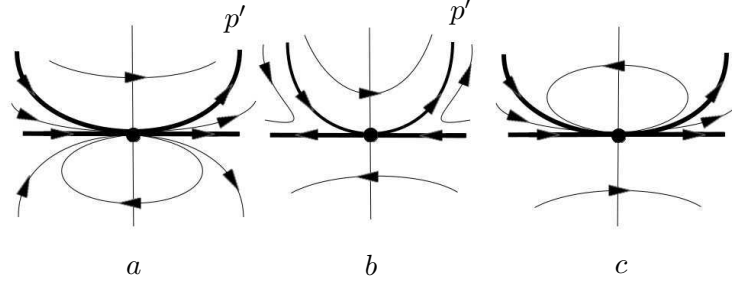


FIGURE 34. Sectorial decomposition of system (26) at the origin. (a) $b > 0$ and $0 < \lambda_2 < \lambda_1 < 2\lambda_2$; or $b < 0$ and $2\lambda_2 < \lambda_1 < \lambda_2 < 0$. If $b > 0$ and $2\lambda_2 < \lambda_1 < \lambda_2 < 0$; or $b < 0$ and $0 < \lambda_2 < \lambda_1 < 2\lambda_2$ then the orientation of the orbits is reversed. The separatrices are contained in $v = u^2$ and in the region $v \leq 0$. (b) $b > 0$ and $0 < 2\lambda_2 < \lambda_1$; or $b < 0$ and $\lambda_1 < 2\lambda_2 < 0$. If $b > 0$ and $\lambda_1 < 2\lambda_2 < 0$; or $b < 0$ and $0 < 2\lambda_2 < \lambda_1$ then the orientation of the orbits is reversed. The separatrices are contained in $v = u^2$ and in $v = 0$. (c) $b > 0, \lambda_2 > 0$ and $\lambda_1 < \lambda_2$; or $b < 0, \lambda_2 < 0$ and $\lambda_1 > \lambda_2$. If $b > 0, \lambda_2 < 0$ and $\lambda_1 > \lambda_2$; or $b < 0, \lambda_2 > 0$ and $\lambda_1 < \lambda_2$ then the orientation of the orbits is reversed. The separatrices are contained in the region $v \geq u^2$ and in $v = 0$.

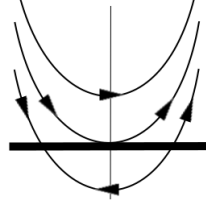


FIGURE 35. Sectorial decomposition of system (26) at the origin. Case $\lambda_1\lambda_2 \neq 0, b(\lambda_1 - \lambda_2) \neq 0, \lambda_1 = 2\lambda_2$ and $b\lambda_2 > 0$. If $\lambda_1\lambda_2 \neq 0, b(\lambda_1 - \lambda_2) \neq 0, \lambda_1 = 2\lambda_2$ and $b\lambda_2 < 0$ then the orientation of the orbits is reversed.

$$\begin{aligned}
 \dot{\bar{u}} &= -c\lambda_2\bar{u}^4\bar{v}^2 + (2c\lambda_2\bar{u}^4 + a(\lambda_1 - \lambda_2)\bar{u}^3 + b(\lambda_1 - \lambda_2)\bar{u}^2)\bar{v} + \\
 &\quad a(2\lambda_2 - \lambda_1)\bar{u}^3 + b(2\lambda_2 - \lambda_1)\bar{u}^2, \\
 \dot{\bar{v}} &= 2c\lambda_2\bar{u}^3\bar{v}^3 + (-2c\lambda_2\bar{u}^3 + a(2\lambda_2 - \lambda_1)\bar{u}^2 + 2b(\lambda_2 - \lambda_1)\bar{u})\bar{v}^2 + \\
 &\quad (a(\lambda_1 - 2\lambda_2)\bar{u}^2 + 2b(\lambda_1 - \lambda_2)\bar{u})\bar{v}.
 \end{aligned}
 \tag{38}$$

After the rescaling given by $ds = \bar{u} dt$ system (38) becomes.

$$\begin{aligned}
\bar{u}' &= -c\lambda_2\bar{u}^3\bar{v}^2 + (2c\lambda_2\bar{u}^3 + a(\lambda_1 - \lambda_2)\bar{u}^2 + b(\lambda_1 - \lambda_2)\bar{u})\bar{v} + \\
&\quad a(2\lambda_2 - \lambda_1)\bar{u}^2 + b(2\lambda_2 - \lambda_1)\bar{u}, \\
\bar{v}' &= 2c\lambda_2\bar{u}^2\bar{v}^3 + (-2c\lambda_2\bar{u}^2 + a(2\lambda_2 - \lambda_1)\bar{u} + 2b(\lambda_2 - \lambda_1)\bar{u})\bar{v}^2 + \\
&\quad (a(\lambda_1 - 2\lambda_2)\bar{u} + 2b(\lambda_1 - \lambda_2))\bar{v}.
\end{aligned}
\tag{39}$$

The singularities (\bar{u}_0, \bar{v}_0) of system (39) with $\bar{u}_0 = 0$ are $(0, 0)$ and $(0, 1)$. **The eigenvalues of the Jacobian matrix of the vector field defined by system system (39) evaluated at $(0, 0)$ and $(0, 1)$ are $b(2\lambda_2 - \lambda_1)$, $2b(\lambda_1 - \lambda_2)$ and $b\lambda_2$, $-2b(\lambda_1 - \lambda_2)$, respectively.**

Observe that the straight line $\bar{v} = 1$ is an invariant of system (39), then the parabola p' is an invariant of system (26). If $u = 0$ and $|v|$ is sufficiently small then the sign of \dot{u} in system (26) is the same than $b(\lambda_1 - \lambda_2)v$. Then we will present only the figures of the blow-up for the case $b > 0$. We summarize the quasi-homogeneous blow-up in the u -direction in Figures 36-38.

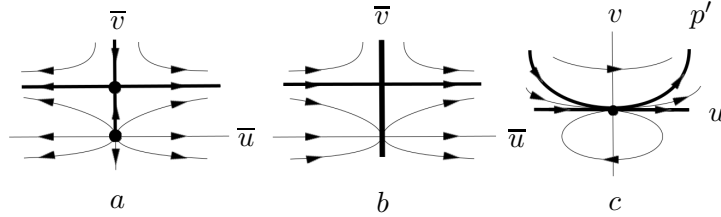


FIGURE 36. Local phase portrait of system (26) at $(0, 0)$ for the case $b > 0$ and $0 < \lambda_2 < \lambda_1 < 2\lambda_2$; or $b < 0$ and $2\lambda_2 < \lambda_1 < \lambda_2 < 0$. If $b > 0$ and $2\lambda_2 < \lambda_1 < \lambda_2 < 0$; or $b < 0$ and $0 < \lambda_2 < \lambda_1 < 2\lambda_2$ then the orientation of the orbits is reversed. (a) System (39). (b) System (38). (c) System (26).

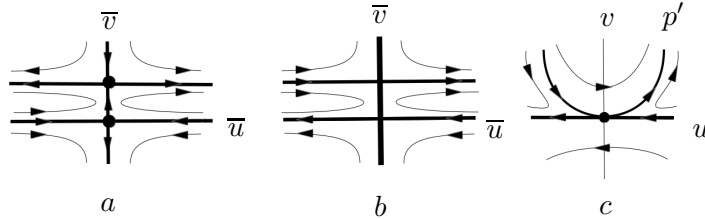


FIGURE 37. Local phase portrait of system (26) at $(0, 0)$ for the case $b > 0$ and $0 < 2\lambda_2 < \lambda_1$; or $b < 0$ and $\lambda_1 < 2\lambda_2 < 0$. If $b > 0$ and $\lambda_1 < 2\lambda_2 < 0$; or $b < 0$ and $0 < 2\lambda_2 < \lambda_1$ then the orientation of the orbits is reversed. (a) System (39). (b) System (38). (c) System (26).

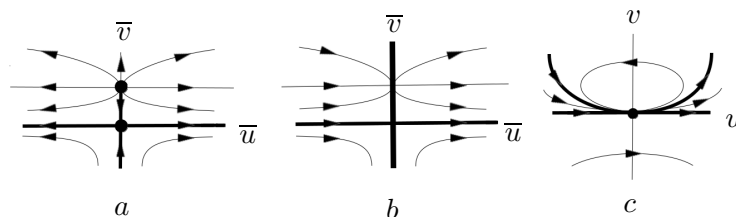


FIGURE 38. Local phase portrait of system (26) at $(0,0)$ for the case $b > 0, \lambda_2 > 0$ and $\lambda_1 < \lambda_2$; or $b < 0, \lambda_2 < 0$ and $\lambda_2 < \lambda_1$. If $b > 0, \lambda_2 < 0$ and $\lambda_2 < \lambda_1$; or $b < 0, \lambda_2 > 0$ and $\lambda_1 < \lambda_2$ then the orientation of the orbits is reversed. (a) System (39). (b) System (38). (c) System (26).

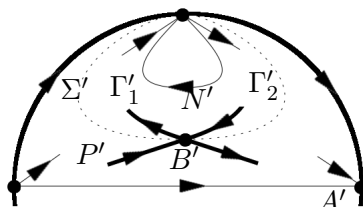


FIGURE 39. Lemma 16.

Case 3.2: $\lambda_1 = 2\lambda_2$. After the rescaling given by $ds = \lambda_2 v dt$ system (26) becomes

$$u' = -cv + 2cu^2 + au + b, \quad v' = 2(cu + a)v + 2bu.$$

Then $u' = b$ when $u = v = 0$ and $v' = 2bu$ when $v = 0$. We present the sectorial decomposition of system (26) at the origin in Figure 35. \square

6. PROOF OF THEOREM 1

Combining the informations of Lemmas 6-15 we obtain the local phase portrait of all the singularities finite and infinite in the Poincaré disc of systems (4) with $\lambda_1^2 + \lambda_2^2 \neq 0$, it is shown in Figure 40. The correspondence between the systems (4) and the local phase portrait in the Poincaré disc shown in Figure 40 is given in Table 1.

Using the **Poincaré-Bendixson** Theorem, the Remarks 3-5 and that we have the invariant parabola $y = x^2$ and the invariant straight line $ax + by + c = 0$, we obtain that each local phase portrait in the Poincaré disc given in Figure 40-a-w, determines a unique global phase portrait in the Poincaré disc of Figure 1-a-w respectively, except for the case given by figures 40-v and 1-v. The proof of the phase portrait in the Poincaré disc of Figure 40-v is given by Figure 1-v follows from the next result.

Lemma 16. *Consider the local phase portrait given in Figure 40-v, which portion corresponding to the region above the line l is shown in Figure 39. Then $\omega(\Gamma'_1)$ and $\alpha(\Gamma'_2)$ are the origin of U_2 .*

Proof. As before for system (4) we denote by P, N and Σ the subsets of \mathbb{R}^2 such that $\dot{x} > 0, \dot{x} < 0$ and $\dot{x} = 0$, respectively. The corresponding subsets in the Poincaré disc are denoted by P', N' and Σ' . In Figure 39 we suppose that $a/b \leq 0$. The case $a/b > 0$ is treated in a similar way.

Since Σ is defined by the equation $b(\lambda_1 - \lambda_2)y = b\lambda_1x^2 + a\lambda_2x + c\lambda_2$, the equation of Σ' in the charts U_1 and U_2 is given by $b(\lambda_1 - \lambda_2)uv = b\lambda_1 + a\lambda_2v + c\lambda_2v^2$ and $b(\lambda_1 - \lambda_2)v = b\lambda_1u^2 + a\lambda_2uv + c\lambda_2v^2$, respectively. Then $A \notin \Sigma'$ and the origin of U_2 is contained in Σ' .

If $\omega(\Gamma_1)$ is different of the origin of U_2 then $\omega(\Gamma_1) = \{A\}$. It follows that $\Gamma_1 \cap N' \neq \emptyset$. This is a contradiction with Lemma 10-(b). \square

REFERENCES

- [1] J.C. ARTÉS AND J. LLIBRE, *Quadratic Hamiltonian vector fields*, J. Differential Equations **107** (1994), 80–95.
- [2] J.C. ARTÉS, J. LLIBRE AND N. VULPE, *Complete geometric invariant study of two classes of quadratic systems*, Electronic J. of Differential Equations **2012**, No. 09 (2012), 1–35.
- [3] N.N. BAUTIN, *On the number of limit cycles which appear with the variation of coefficients from an equilibrium position of focus or center type*, Mat. Sbornik **30** (1952), 181–196, Amer. Math. Soc. Transl. Vol. 100 (1954), 1–19.
- [4] L. CAIRÓ, J. LLIBRE, *Darbouxian first integrals and invariants for real quadratic systems having an invariant conic*, J. Physics A: Math. Gen. **35** (2002), 589–608.
- [5] T. DATE, *Classification and analysis of two-dimensional homogeneous quadratic differential equations systems*, J. of Differential Equations **32** (1979), 311–334.
- [6] H. DULAC, *Détermination et intégration d'une certaine classe d'équations différentielle ayant par point singulier un centre*, Bull. Sci. Math. Sér. (2) **32** (1908), 230–252.
- [7] F. DUMORTIER, J. LLIBRE AND J.C. ARTÉS, *Qualitative theory of planar differential systems*, Universitext, Springer-Verlag, 2006.
- [8] YU.F. KALIN AND N.I. VULPE, *Affine-invariant conditions for the topological discrimination of quadratic Hamiltonian differential systems*, Differential Equations **34** (1998), no. 3, 297–301.
- [9] W. KAPTEYN, *On the midpoints of integral curves of differential equations of the first degree*, Nederl. Akad. Wetensch. Verslag. Afd. Natuurk. Koninkl. Nederland (1911), 1446–1457 (Dutch).
- [10] W. KAPTEYN, *New investigations on the midpoints of integrals of differential equations of the first degree*, Nederl. Akad. Wetensch. Verslag Afd. Natuurk. **20** (1912), 1354–1365; **21**, 27–33 (Dutch).
- [11] N. A. KOROL, “The integral curves of a certain differential equation”, (in Russian), Minsk. Gos. Ped. Inst. Minsk (1973), 47–51.
- [12] M.A. LIAPUNOV *Problème général de la stabilité du mouvement*, Ann. of Math. Stud. **17**, Princeton University Press, 1947.

- [13] J. LLIBRE AND M.F. DA SILVA, *Global phase portraits of Kukles differential systems with homogenous polynomial nonlinearities of degree 6 having a center and their small limit cycles*, Int. J. of Bifurcation and Chaos **26** (2016), 1650044, 25 pp.
- [14] J. LLIBRE AND J. YU, *Phase portraits of quadratic systems with an ellipse and a straight line as invariant algebraic curves*, Electronic J. of Differential Equations **2015**, N 314, 14 pp.
- [15] V.A. LUNKEVICH AND K. S. SIBIRSKII, *Integrals of a general quadratic differential system in cases of a center*, Differential Equations **18** (1982), 563–568.
- [16] L.S. LYAGINA, *The integral curves of the equation $y' = (ax^2 + bxy + cy^2)/(dx^2 + exy + fy^2)$* (in Russian), Usp. Mat. Nauk, **6-2(42)** (1951), 171–183.
- [17] L. MARKUS, *Quadratic differential equations and non-associative algebras*, Annals of Mathematics Studies, Vol **45**, Princeton University Press, 1960, pp 185–213.
- [18] T. A. NEWTON *Two dimensional homogeneous quadratic differential systems*, SIAM Review **20** (1978), 120–138.
- [19] H. POINCARÉ, *Mémoire sur les courbes définies par les équations différentielles*, Journal de Mathématiques **37** (1881), 375–422; Oeuvres de Henri Poincaré, vol. I, Gauthier-Villars, Paris, 1951, pp 3–84.
- [20] J.W. REYN, *Phase portraits of planar quadratic systems*, Mathematics and Its Applications (Springer), **583**, Springer, New York, 2007.
- [21] D. SCHLOMIUK, *Algebraic particular integrals, integrability and the problem of the center*, Trans. Amer. Math. Soc. **338** (1993), 799–841.
- [22] K. S. SIBIRSKII AND N. I. VULPE, *Geometric classification of quadratic differential systems*, Differential Equations **13** (1977), 548–556.
- [23] E. V. VDOVINA, *Classification of singular points of the equation $y' = (a_0x^2 + a_1xy + a_2y^2)/(b_0x^2 + b_1xy + b_2y^2)$ by Forster's method* (in Russian), Differential Equations **20** (1984), 1809–1813.
- [24] YE YANQIAN AND OTHERS, *Theory of Limit Cycles*, Transl. Math. Monographs **66**, Amer. Math. Soc., Providence, 1984.
- [25] YE YANQIAN, *Qualitative Theory of Polynomial Differential Systems*, Shanghai Scientific & Technical Publishers, Shanghai, 1995 (in Chinese).
- [26] WEI YIN YE AND YE YANQIAN, *On the conditions of a center and general integrals of quadratic differential systems*, Acta Math. Sin. (Engl. Ser.) **17** (2001), 229–236.
- [27] N. I. VULPE, *Affine-invariant conditions for the topological discrimination of quadratic systems with a center*, Differential Equations **19** (1983), 273–280.
- [28] H. ŻOŁĄDEK, *Quadratic systems with center and their perturbations*, J. Differential Equations **109** (1994), 223–273.

¹ DEPARTAMENT DE MATEMÀTIQUES, UNIVERSITAT AUTÓNOMA DE BARCELONA, 08193 BELLATERRA, BARCELONA, CATALONIA, SPAIN

E-mail address: jllibre@mat.uab.cat

² DEPARTAMENTO DE MATEMÁTICA, UNIVERSIDADE FEDERAL DE SANTA MARIA, 97110-820, SANTA MARIA, RS, BRAZIL

E-mail address: mauriciofronzadasilva@hotmail.com

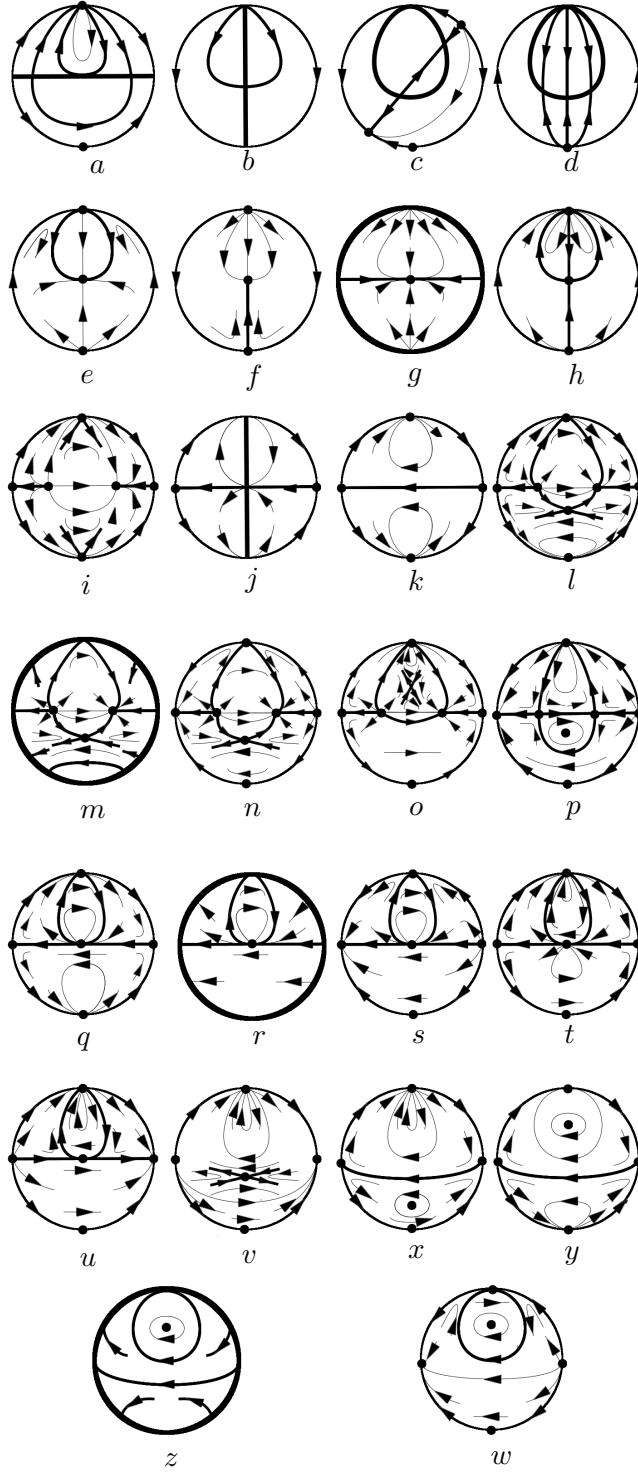


FIGURE 40. Local phase portraits in the Poincaré disc of systems (4).